Stony Brook University

Fluorescence-based Approaches for Studying Nucleotide Excision Repair

A Thesis Presented

by

Andy Chong Kit Khoo

to

The Graduate School

in Partial Fulfillment of the

Requirements

for the Degree of

Master of Science

in

Chemistry

Stony Brook University

December 2011

Stony Brook University

The Graduate School

Andy Chong Kit Khoo

We, the thesis committee for the above candidate for the

Master of Science degree, hereby recommend

acceptance of this thesis.

Orlando D. Schärer, Ph.D. – Dissertation Advisor
Professor, Department of Pharmacological Sciences

Elizabeth M. Boon, Ph.D. – Chairperson of Defense
Professor, Department of Chemistry

Carlos Simmerling, Ph.D.
Professor, Department of Chemistry

This thesis is accepted by the Graduate School

Lawrence Martin
Dean of the Graduate School

ii

Abstract of the Thesis

Fluorescence-based Approaches for Studying Nucleotide Excision Repair

by

Andy Chong Kit Khoo

Master of Science

in

Chemistry

Stony Brook University

2011

Nucleotide excision repair (NER) is a versatile DNA repair pathway known for its wide substrate specificity. NER is able to recognize and remove a variety of helix distorting DNA lesions including those induced by ultraviolet (UV) light, various environmental mutagens and chemotherapeutic agents. The importance of NER is underscored by the inherited human disorder xeroderma pigmentosum (XP), which is caused by the deficiency of genes that are involved in NER. The characteristics of XP patients include an extreme sensitivity to UV light and a more than 2000-fold increased incidence of skin cancer. NER works through a "cut and patch" mechanism that involves the excision of a 24-32mer oligonucleotide containing the damage and restoration the original sequence of the DNA through repair synthesis using the non-damaged strand as the template. NER involves the concerted action of over 30 proteins that work in a sequential order. The rate of repair by NER depends on the degree of duplex destabilization induced by a lesion. Repair rates have been determined using two types of *in-vitro* NER assays that require the use of radioactive materials to label and detect NER products. The limitations of using of radioactive materials include the short shelf life of substrates, as well as laborious and cumbersome procedures involved in their preparation. More importantly, currently used *in-vitro* assays are only able to detect NER products, but not the intermediates or unreacted substrates.

The work of this thesis was focused on developing innovative NER assays that combine the advantages of the traditionally used *in-vitro* NER assays, while overcoming the limitation of

using radioactive materials. Our approach was to develop two new NER assays using the incorporation of fluorescent tags via oxime formation and click-chemistry to label NER substrates and products. The advantages of using fluorescent labeling include circumventing issues associated with the use of radioactivity, achieving shorter exposure time and longer lifespan of substrates. Our results suggest that click chemistry in particular holds great promise for successfully use in NER assays. These new fluorescent substrates described in this thesis should be valuable tools for studies of the NER pathway since they will allow for the quantitative determination of NER rates and the visualization of various steps of the NER reaction.

Table of Contents

List of Abbreviations

AABP	Acetylaminobenzophenone
AAF	Acetylaminofluorene
AF	Aminofluorene
CEP	2-cyanoethyl-N,N-diisopropylphosphoramidite
CS	Cockayne syndrome
$CuSO_4$	Copper(II)sulfate
DMTr	4, 4-dimethoxytrityl group
DNA	Deoxyribonucleic acid
ds DNA	Double stranded DNA
GG-NER	Global genome – nucleotide excision repair
NER	Nucleotide excision repair
ss DNA	Single stranded DNA
TBTA	Tris(benzyltriazolylmethyl)amine
TC –NER	Transcription coupled - nucleotide excision repair
TFIIH	Transcription factor IIH
THPTA	Tris-(3-hydroxypropyl triazolylmethyl)-amine
TTD	Trichothiodystrophy
XP	Xeroderma pigmentosum

Acknowledgments

First and foremost, I would like to express my sincere gratitude towards Dr. Orlando Schärer, my advisor, for giving me the opportunity to work in his research group and on this interesting project. He has been extremely encouraging and supportive of my work. By far, he is one of the most approachable advisors from whom I learnt many research skills. Moreover, I would like to extend my appreciation towards my thesis committees, Dr. Elizabeth Boon and Dr. Carlos Simmerling, for their advice, time and support.

During my stay in lab, I came to know my fellow group members: Barbara, Angelo, AJ and Banke. I would like to thank all of them for their ideas, support and encouragement. My heartfelt gratitude towards Jung-Eun Yeo, who mentored me and taught me both biochemistry techniques and organic synthesis; Thank you for everything! In addition, I would like to thank my current colleagues in the lab, Shivam, Yan, Burak, Alejandra and Grace for their help and discussions over the years of my degree.

During the past two years of my graduate life, I made new friends along the way: Bora, Sonam, Justin, Yueming, Carla and my other classmates. I will always remember our study sessions and the times when we shared our ups and downs. Life seems to be impossible without my best friends, Cheok Hoong and Brian On, thank you for always being there for me! Your encouragement and advice has always motivated me.

Last but not least, I owe my deepest gratitude to my family. I strongly believe that without them, I would not be where I am today. Their continuous support means the world to me, and their faith in me made me the person I am today. Thank you, Mom and Dad! I love you! My brothers, Gary and Eric, thank you for your constant support and always cheering me up.

Chapter 1

1.1 Introduction

Deoxyribonucleic acid (DNA) is the carrier of genetic information, which is passed across generations. The sequence and integrity of DNA needs to be maintained as it encodes the proteins that control cellular proliferation and function in all living organisms. Although DNA is fairly stable, its integrity is constantly challenged by replication errors, different kinds of endogenous factors such as oxygen radicals and reactive metabolites, and exogenous factors such as environmental mutagens, ionization radiation and ultraviolet (UV) light [1]. The estimated number of damaging events occurring in a single cell may range from 10^5-10^6 per day [2]. In the short term, DNA damage can lead to the disruption of normal cell cycle regulation and gene-expression by blocking DNA replication and transcription activities. Furthermore, the prolonged effects of damage to DNA can lead to mutations, which alter the coding sequence of DNA and permanently change the genetic information [3]. As a result, damage to DNA is associated with cancer and premature aging in humans. To counteract the modifications of DNA and to preserve the genomic integrity, cells have evolved several defense mechanisms that include signaling and DNA repair pathways (Scheme 1) [4].
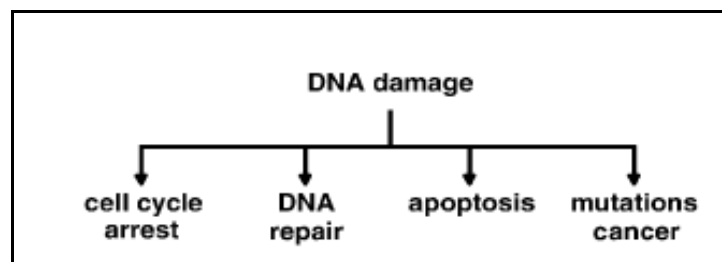
Scheme 1: Responses to and consequences of DNA damage [4].

In the response to DNA damage, signaling pathways known as DNA damage checkpoints are activated that temporarily arrest the cell cycle, thereby providing enough time to repair DNA damage before proceeding with replication and cell division [4,5]. If the DNA damage load is too high and cannot be eliminated successfully, the cell may undergo programmed cell death (apoptosis). On the other hand, the persistence of DNA lesions may lead to the accumulation of mutations and cellular transformation, eventually leading to tumor formation [1]. In addition to cell-cycle arrest and apoptotic responses, cells have also evolved five major repair pathways that address different lesions caused by a variety of agents (Figure 1) [4]. The work of this thesis was focused on investigating one of these pathways, nucleotide excision repair (NER), which is able to recognize and remove a large variety of bulky adducts.
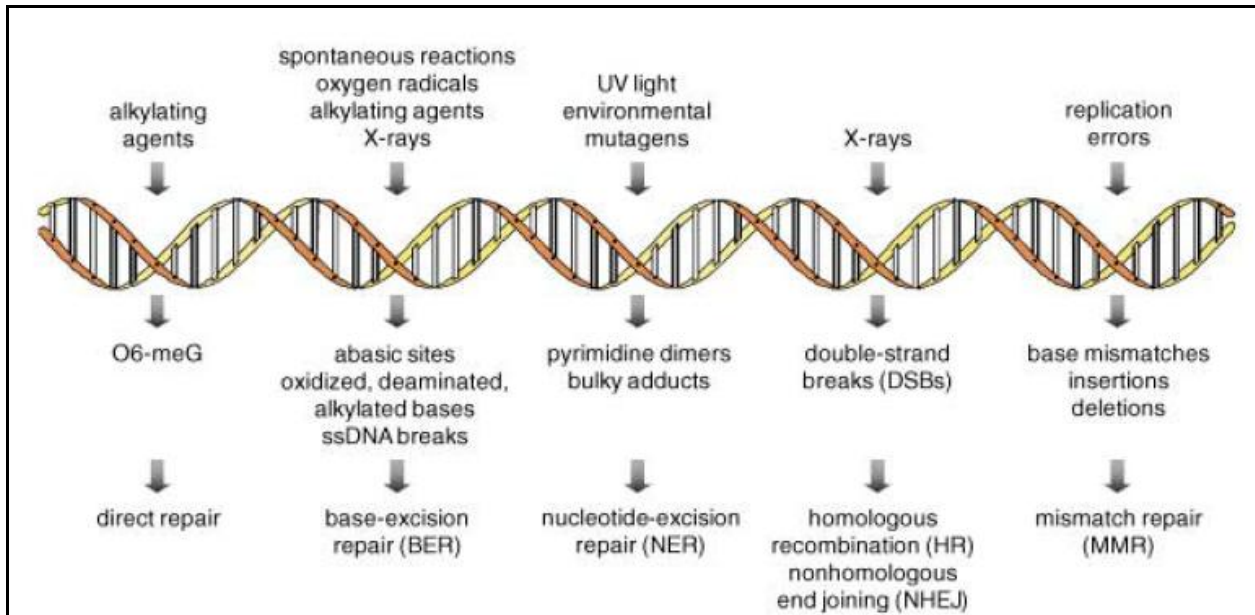

Figure 1: Most common DNA-damaging agents, lesions, and repair pathways [4].

2

1.2 Nucleotide excision repair

Nucleotide excision repair (NER) is a versatile DNA repair pathway known for its wide substrate specificity. NER is able to recognize and remove a variety of helix distorting DNA lesions including those induced by UV light, various environmental mutagens and chemotherapeutic agents [1]. NER has two distinct subpathways, global genome NER (GG-NER), and transcription coupled NER (TC-NER). The difference between these two subpathways is the damage recognition step, which depends on the location of DNA lesion in the genome, and on specialized recognition factors that are responsible for detecting the damage [1,6,7]. GG-NER is initiated by the binding of UV-DDB and/or XPC-RAD23B protein complexes to helix-distorting DNA lesion in any location of the genome. On the other hand, TC-NER is triggered by a stalled RNA polymerase II in the elongation mode at lesions on the transcribed DNA strand of active genes [1,6,7]. People with defects in NER genes suffer from human genetic diseases such as xeroderma pigmentosum (XP), Cockayne syndrome (CS), and trichothiodystrophy (TTD) [1,8]. XP patients are incapable of removing bulky lesions from their DNA, and are extremely sensitive to UV light. As a result, they have more than 2000-fold increased incidence of skin cancer. These XP patients have been classified into eight complementation groups (XP-A to XP-G) with respect to the deficiency of genes that are involved in NER. A last complementation group known as the variant form of XP (XP-V) has defects in DNA polymerase η, a Y-family polymerase that is specialized for translesion synthesis (TLS) past UV-induced DNA lesions [9]. Although CS and TTD patients are not cancer prone, they suffer from various developmental abnormalities and shorter life expectancy, due to an impairment of some aspect of transcriptions [1,8]. The severity of these diseases has urged studies to elucidate the detailed mechanism of NER repair with the hope to have better

understanding of the human disorders and carcinogenesis. Furthermore, as NER contributes to a resistance against antitumor agents such as cisplatin that damage the DNA, it is also a potential target for anti-tumor therapy.

1.3 Molecular mechanism of the Nucleotide Excision Repair

NER works through a "cut and patch" mechanism and excises a 24-32mer oligonucleotide containing the damage, and restores the original sequence of the DNA through repair synthesis using the non-damaged strand as the template. NER involves the concerted action of over 30 proteins that work in a sequential order [10]. NER is initiated by the XPC-RAD23B protein complex [11,12], (Figure 2 A), which has the ability to recognize bulky damages that cause severe distortion of the DNA duplex. The binding affinity of XPC-RAD23B is highly correlated with degree of distortion and thermodynamic destabilization of the DNA duplex induced by the lesion [1]. More specifically, XPC-RAD23B has been shown to have a high binding affinity for UV adducts such as pyrimidine (6-4) pyrimidone (6-4PPs), acetylaminofluorene adducts (dG-AAF), and benzo[a]pyrene (B[a]P) [1]. By contrast, XPC-RAD23B does not bind less distorting lesions such as cyclopyrimidine dimers (CPDs) as well, and NER needs the help of the another proteins, DDB1/DDB2 for damage recognition of less distorting lesions [13]. Fortunately, the understanding of the binding mechanism of XPC-RAD23B to the damaged DNA has became better understood through the solution of the crystal structure of *Saccharomyces cerevisiae* RAD4, the yeast homolog of XPC, bound to DNA containing a CPD lesion [14]. In this structure, RAD4 was found to bind to the non-damaged strand opposite to the lesion rather than the lesion itself, which is consistent with the findings of XPC-RAD23B being able to distinguish a wide range of DNA lesions from non-damaged DNA.

4

After the recognition of XPC-RAD23B, the ten subunit transcription and repair factor TFIIH is recruited to the damage site via protein-protein interactions (Figure 2 B). TFIIH contains two ATP dependent helicase subunits, XPB and XPD, which partially open the DNA helix around the damaged site [15], and also serve as the damage verification factor [16]. Experimental data has supported a role for XPB to pry open the DNA around the lesion, while XPD tracks along the DNA with a 5' to 3' polarity until it is blocked by a lesion, confirming the presence of a lesion containing the chemical modification [16]. Full opening of the DNA duplex and stable preincision complex formation is achieved after recruitment of XPA, RPA and XPG to the damaged site, simultaneous with the dissociation of XPC-RAD23B (Figure 2 C) [10,17]. XPA is a small protein that helps to stabilize the pre-incision complex, and interacts with the single-stranded DNA binding protein RPA. RPA is believed to bind to the non-damaged DNA where it helps to position the two endonucleases ERCC1-XPF and XPG [18]. The second endonuclease ERCC1-XPF is the last protein to be recruited to the damage site via its interaction with XPA [19]. Once the proper assembly of pre-incision complex is established, the dual incisions are carried out by ERCC1-XPF and XPG that cleave the DNA 5' and 3' to the lesion respectively (Figure 2: D and E) [20,21,22,23]. The NER pathway is completed by DNA polymerases δ, ε, or κ and associated factors that fill in the gap, and DNA ligase I or IIIα that seal the nick, and restore the DNA to its undamaged form (Figure 2 F) [24].
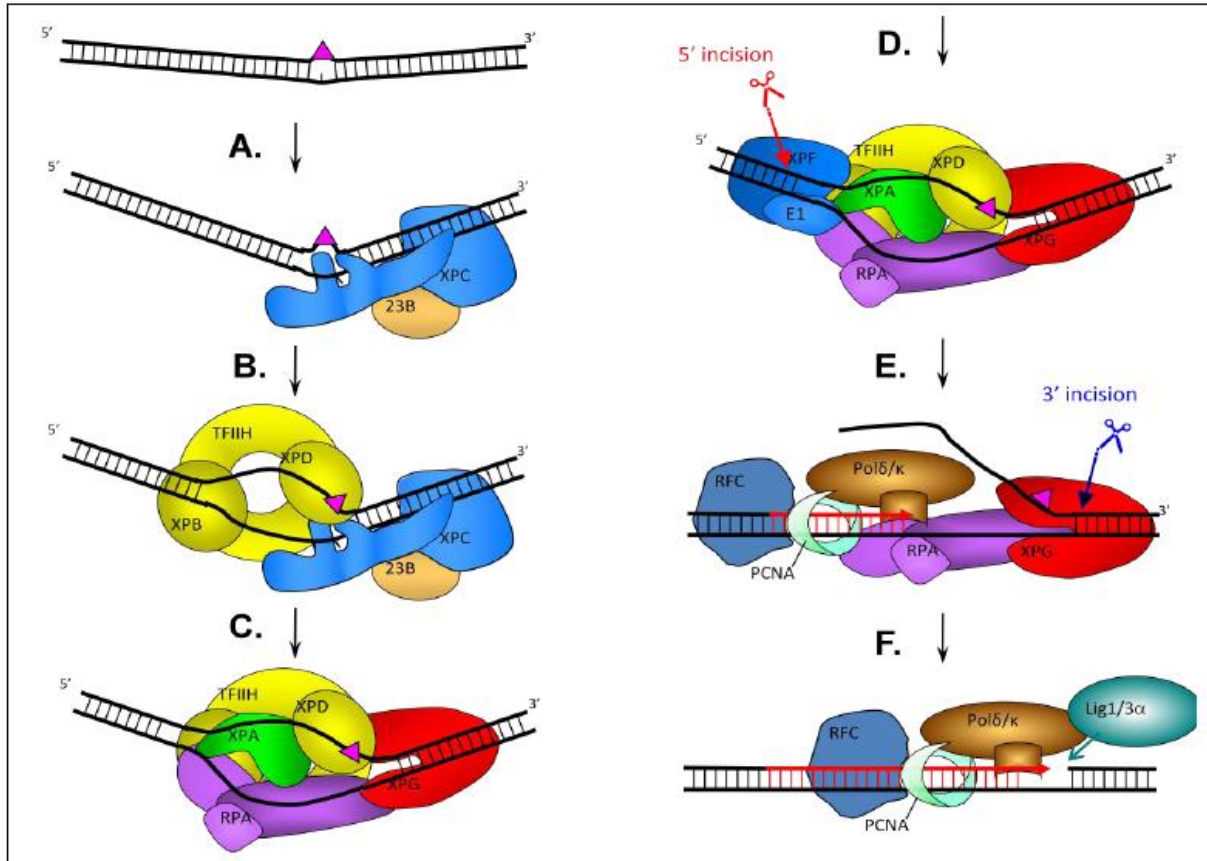
Figure 2: Model for the nucleotide excision repair (NER) pathway. XPC-RAD23B binds to the undamaged strand of DNA (A), allowing the recruitment of TFIIH (B). The verification step is achieved by stalling of XPD at the lesion which allows the formation of the preincision complex by recruitment of XPA, RPA and XPG (C). ERCC1-XPF is recruited to the preincision complex via interaction with XPA, leading to 5' incision to the lesion (D). The presence of free 3'-OH initiates the repair synthesis by the replication machinery, Pol δ/κ, and associated factors, and thus triggers the 3' incision to the lesion by XPG (E). The resulted nick is sealed by DNA ligase IIIα or ligase I to complete the NER pathway.

1.4 DNA lesions repaired by nucleotide excision repair pathway

One of the most remarkable features of nucleotide excision repair pathway is its ability to recognize and repair a wide variety of structurally unrelated DNA lesions such as those induced by UV radiation from sunlight, or exposure to carcinogenic chemicals such as cisplatin, polycyclic aromatic hydrocarbons and heterocyclic aromatic amines [1]. Table 1 provides examples of such DNA adducts.
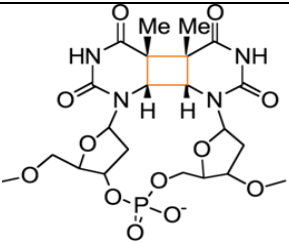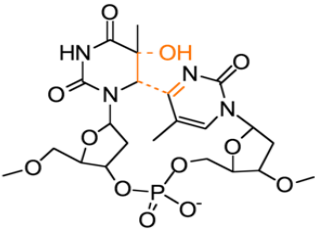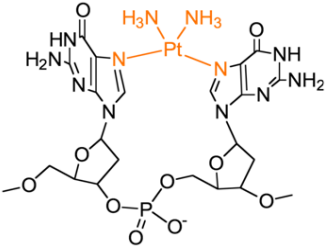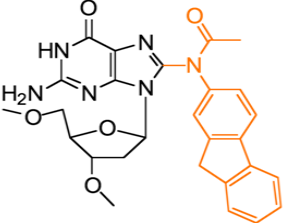
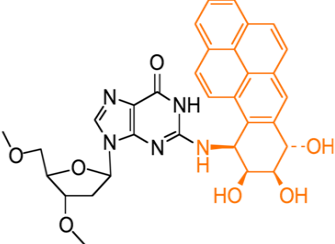| DNA adducts	Properties
 Cyclobutane Pyrimidine Dimers (CPDs)	• Formed upon exposure to UV radiation. • Formed by a [2+2] cycloaddition reaction of the C5-C6 double bonds of adjacent pyrimidines bases. • CPDs adducts can form between adjacent TT, TC, CT or CC depending on the wavelengths of irradiation and adjacent sequences.
 Pyrimidine (6-4) pyrimdone (6-4PP)	• Formed upon exposure to UV radiation. • Formed by a [2+2] cycloaddition reaction of the C5-C6 double bond of a 5' pyrimidine base and the C4 carbonyl group of a 3' thymine. • 6-4PPs adducts can formed between adjacent TC, TT or CC depending on the wavelengths of irradiation and adjacent sequences.
 Cisplatin 1,2-d(GpG) intra	• Activated when the labile chloride ligands of cisplatin are substituted by a hydroxide ion in low salt concentration, to form hydrolyzed cisplatin, an activated electrophilic derivative of cisplatin that reacts with nucleophilic sites on DNA. • Intrastrand (N7-N7) crosslinks: 1,2-d(GpG), 1,2-d(ApG) and 1,3-d(GpNpG) adducts.
 Acetylaminofluorene (dG-AAF)	• Activated during the metabolic detoxification of aminofluorene in the body. • Aromatic amines are transformed into reactive arylnitrenium intermediates that form adducts with C8 or N^2 of dG. • The possible mutagenic arylamine adducts: dG-AAF, dG-AF or dG-N^2-AAF.
 Benzo[a]pyrene (dG-B[a]P)	• Activated during the metabolic detoxification of Benzo[a]pyrene in the body. • Aromatic hydrocarbons are converted into eletrophilic epoxides, and react with the exocyclic amino groups of adenine and guanine. • The possible aromatic hydrocarbon adducts: 10*S* (+)-*trans-anti*-[BP]-N^2-dG or 10*S* (+)-*trans*-B[a]P-dG and various stereoisomers.

Table 1: Examples of DNA adducts formed by UV irradiation and carcinogenic chemicals [1]. Abbreviations: T: Thymine; C: Cytosine; A: Adenine; G: Guanine; B[a]P: benzo[a]pyrene, AF: aminofluorene; AAF: acetylaminofluorene.

Although these DNA adducts have distinct primary structures, the common feature recognized by NER is that they create some degree of distortion and thermodynamic destabilization of the DNA duplex. The main criterion if DNA substrates are targeted by NER is the base-pairing disruption that is induced by a chemical modification [16]. For example, modified deoxyribose phosphate backbones that sustain the Watson-Crick base pairing are not processed as lesions by NER, unless they are placed in a bubble containing mismatched base-pairs that destabilize the DNA duplex [25]. As a result, a "bipartite substrate discrimination" model was proposed to indicate that damage recognition in NER occurs in two distinct steps: recognition of the destabilization induced by the lesion and verification step of the presence of a chemical modification [16,26]. This model is consistent with the observation that lesions that induce a higher degree of helix destabilization are recognized and repaired more efficiently by NER. This is evident, for examples, from the higher repair rates displayed by 1,3-d(GnNpG) versus 1,2-d(GpG) intrastrand cisplatin cross-links, or dG-AAF versus dG-AF adducts [1]. These studies of repair rate have been determined using conventional *in-vitro* NER assays that require the use of radioactive materials to label and detect NER products.

1.5 Conventional *in-vitro* NER repair assays

To date, there are two main *in vitro* NER assays that have been used to elucidate the molecular mechanism of NER in considerable detail. The first assay, developed by Sancar and co-workers, used an internal labeling strategy to allow the direct monitoring of the excision step of the NER reaction: A short oligonucleotide containing a unique lesion was 5' radiolabeled with ^{32}P prior to incorporation into plasmid by primer extension or into a linear double-stranded DNA of about 140 base pairs by ligation. The excised NER products of 24- to 32-nucleotide fragments

containing the lesion and the internal ^{32}P label were detected by autoradiography (Figure 3a) [27]. Although this assay allows for the direct monitoring of the excised NER products and the quantification of the yield of the reaction, a major drawback is the radioactive decay of ^{32}P, which limits the shelf-life of the substrates. Another drawback of this assay is that the preparation of the internally radiolabeled NER substrates is laborious and cumbersome. The second *in-vitro* NER assay, developed by Woods and co-workers, used a post-labeling method to detect the NER excision products: A plasmid containing a site-specific lesion is incubated with a NER proficient cell-extract resulting in the release of a product of 24-32- nucleotides are containing the lesion. The excised NER fragments are annealed to a complementary strand containing a four guanosine overhang, and is labeled by a fill-in reaction with α-[^{32}P]- dCTP and a DNA polymerase (Figure 3b) [28].
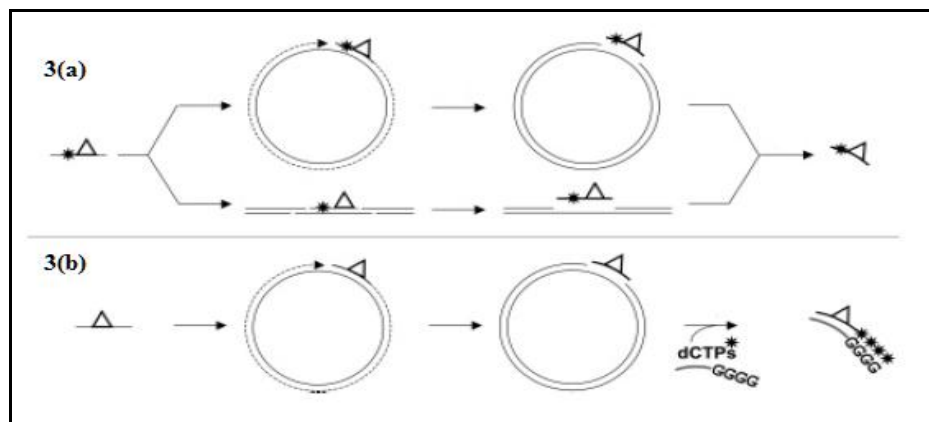

Figure 3: Strategies used for substrate preparation and investigation of the NER reactions *in vitro* [1]. 3(a) the direct detection of excised NER products using internal radiolabeled phosphate strategy. A short oligonucleotide is 5' radiolabel with ^{32}P prior to incorporate into a plasmid by either primer extension protocol to produce circular-closed plasmid, or by ligation reaction into a long linear double-stranded DNA. The excised products containing the internal radiolabeled phosphate near the lesion are detected by autoradiography. **3(b)** the detection of excised NER products via post-labeling method. A plasmid containing a site-specific lesion is prepared by annealing of a 5' phosphorylated oligonucleotide containing a lesion, and by primer extension reaction. This plasmid containing a site-specific lesion is incubated with HeLa cell extract, and the NER excised fragments of 24-32 nucleotides are detected by annealing a complementary oligonucleotide containing a non-complementary 4Guanosine overhang and filling in with [α-^{32}P] dCTP.

The advantage of this assay is that it uses an indefinitely stable substrate, which can be stored and used whenever it is convenient. A flipside of this assay is that the determination of the accurate reaction yield is not straightforward, as NER products but not unreacted plasmids or partially incised products are detected.

1.6 Development of a new NER *in-vitro* assay with non-radioactive labeling strategy

The work of this thesis was focused on developing an innovative approach to monitor NER by combining the advantages of two currently used *in-vitro* NER assays, while overcoming the limitation associates with the use of radioactive materials. Our goal was to develop two new NER assays using incorporation of fluorescent tags via oxime formation and click-chemistry into NER substrates and products. The advantages of using fluorescent labeling include circumventing issues associated with radioactivity, achieving shorter exposure time and longer life-span of substrates.

The first strategy was to fluorescently label a substrate that is a derivative of the known NER substrate, dG-AAF prior to incorporation into a plasmid. Plasmids containing a labeled damage would then be used in the NER assays followed by the direct monitoring the excised fragments by fluorescence (Figure 4). The design of the NER substrate that will be used for this labeling strategy is based on the observation that the aromatic moiety of dG-AAF can be replaced with a different aromatic group while retaining active as a NER substrate. A former group member, Ludovic Gillet conducted an *in-vitro* assay by incubating the plasmids containing the dG-AAF adduct, and its derivative which has the fluorene group replaced with an aminobenzophenone group, (dG-AABP). The dG-AABP substrate was found to be repaired with

equal NER efficiency as dG-AAF, thus indicating dG-AABP is a potent NER substrate (Figure 5).
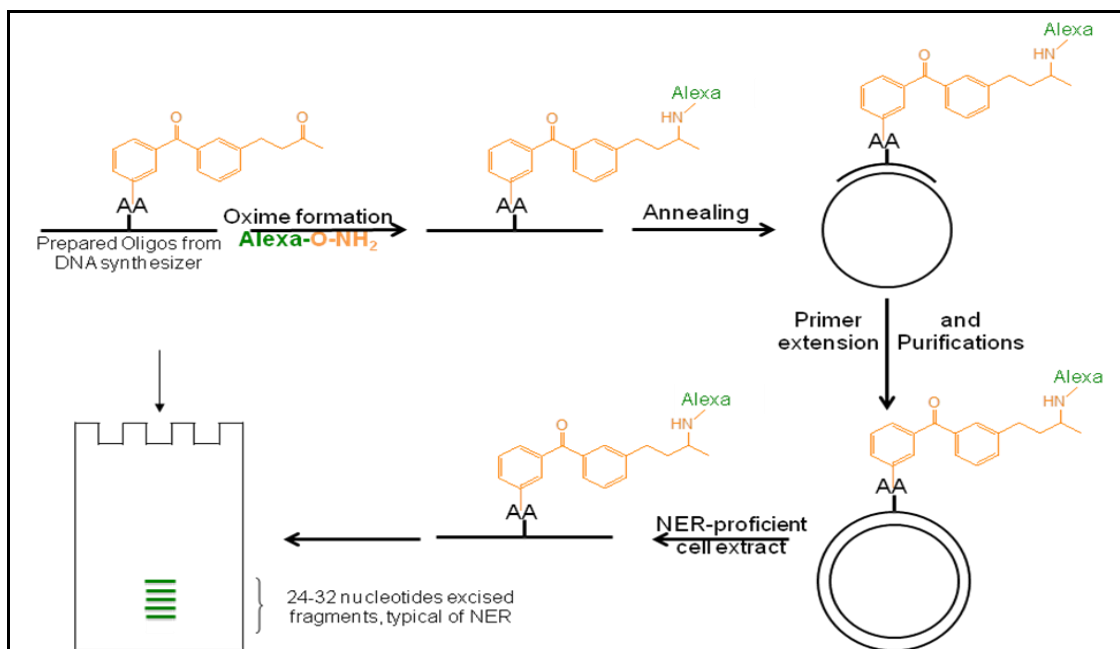

Figure 4: A scheme to prepare NER substrate and monitor excised NER fragments via pre-labeling method. A short oligonucleotide containing a site-specific lesion is pre-labeled with an Alexa hydroxylamine via oxime formation, and the oligonucleotide is annealed to a single-stranded DNA, and followed by primer extension protocol. The plasmid containing a site-specific lesion is purified over EtBr/CsCl gradient, and incubated with a proficient HeLa cell extract. The NER excised products of 24-32 nucleotides are resolved and visualized on a sequencing gel, and detected by fluorescence detection (abbreviation: AA: dG-acetyl-amino).
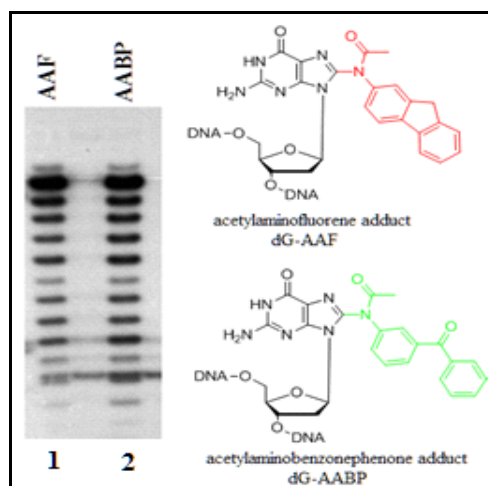

Figure 5: The AAF derivative AABP is a potent NER substrate (data excerpted from a former member, Ludovic Gillet's PhD dissertation [29]). Plasmids containing a lesion, dG-AAF, and its derivative dG-AABP were incubated with NER proficient HeLa cell extract. The excised products were analyzed and detected via post-labeling method as describe in figure 3b.

11

Based on these studies, we thought that a dG-AABP analog containing a substituent such as butan-3-one linker could serve as a handle to tag the products with commercially available hydroxylamine fluorescent dyes via oxime formation without affecting NER activity (Figure 6).
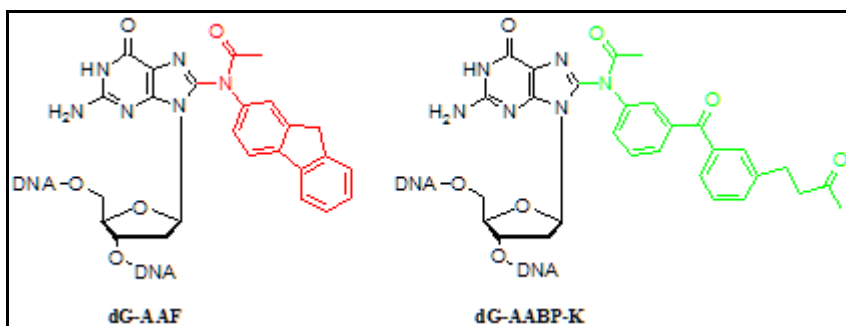

Figure 6: The structures of dG-AAF (dG-acetylaminofluorene) and its derivative, dG-AABP-K (dG-acetyl-aminobenzophenone-ketone).

The advantage of having a new NER fluorescent substrate is that it will greatly facilitate the quantitative measurement of the excised NER products using a Typhoon imaging system. In addition, it will be possible to detect unreacted substrates and partially incised reaction intermediates by digestion of the plasmid with restriction enzymes. We will also use fluorescent NER substrate to address the controversial issue of the order of the two incision steps in NER [15,23,30]. Previous studies have shown that XPG was able to perform an uncoupled 3' incision, in the absence of ERCC1-XPF in a cell extract [15,30], while more recent studies from our laboratory have indicated that ERCC1-XPF cleaves 5' to the lesion first, followed by 3' incision by XPG [23]. The availability of fluorescent NER substrates will make it possible to resolve this controversy by simultaneously detecting the substrate, dual incision product, as well as the two single 5' or 3' incision products.

We also aimed to develop a second non-radioactive labeling strategy to monitor NER fragments by incubating a reactive group adjacent to the lesion that will be labeled with a fluorescent dye after the NER reaction. For this purpose, a site-specific lesion, dG-AAF will be

placed in an oligonucleotide next to a 5-ethynylthymidine (EdU) residue and incorporated into a plasmid using a primer extension reaction. The plasmid will then be incubated with a NER proficient cell-extract to release products containing an alkyne functional group and the damage. Finally, these fragments will be labeled with a commercially available azide fluorescent dye via click chemistry (Figure 7).
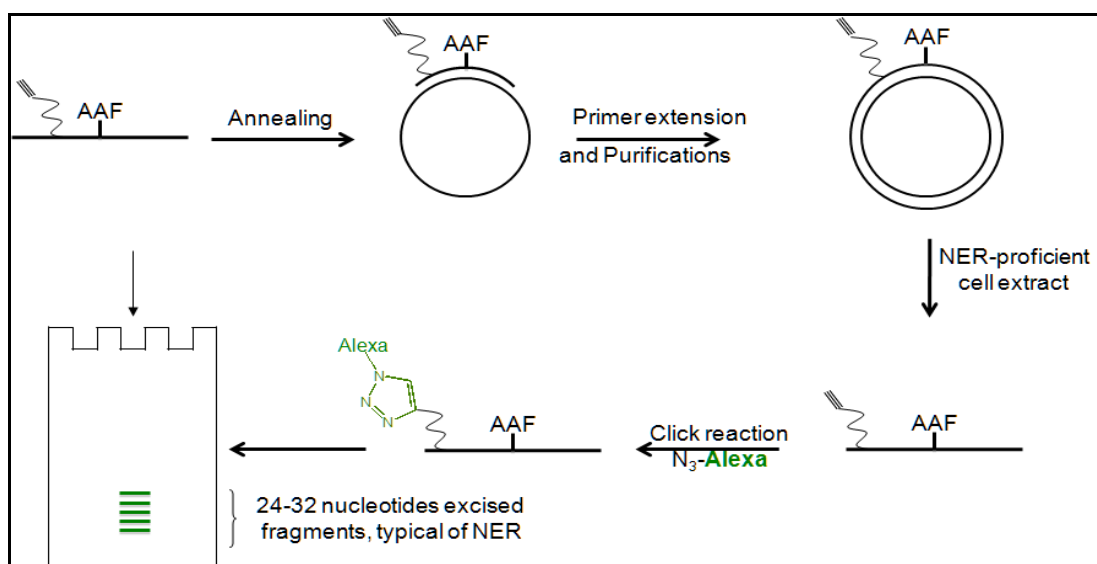

Figure 7: A scheme to prepare NER substrate and monitor excised NER fragments via post-labeling method. A short oligonucleotide containing a site-specific lesion and alkyne functional group is annealed to a single-stranded DNA, and followed by primer extension protocol. The plasmid containing a site-specific lesion is purified over EtBr/CsCl gradient, and incubated with a proficient HeLa cell extract. The NER products of 24-32 nucleotides containing damage and alkyne group are fluorescently labeled with azide fluorescent dye via click chemistry. Those fragments are resolved and visualized on a sequencing gel, and detected by fluorescence detection. Abbreviation: AAF: 2-acetyl-aminofluorene.

The term "click chemistry" refers to a set of reactions that occur with high yield and selectivity under ambient conditions [31]. One of the most well-recognized examples of is the copper (I)-catalyzed, [3+2] cycloaddition between alkyne and azide functional groups [32]. The reasons for utilizing the azide and alkyne groups are that they undergo a highly selective reaction in the presence of Cu(I), while being entirely unreactive to other common functional groups in biological samples [33]. Furthermore, these functional groups are small in size which makes

them ideal to label biomolecules without significantly perturbing the structure of DNA and proteins [34]. Click chemistry has been effectively used to label oligonucleotides for various purposes [35]. To synthesize the substrates needed for this approach, a phosphoramidite building block for 5-ethynyl-dU (EdU) that is available commercially from Glen Research and Berry & Associates, which will be incorporated to oligonucleotides along with dG-AAF lesions. Since the EdU is almost isosteric to thymine, it is not expected to interfere with the NER reaction. A former group member, Jung-Eun Yeo performed *in-vitro* assays with plasmids containing dG-AAF and EdU or dG-AAF or EdU only using radioactive detection of the substrates (Figure 8). While plasmid containing dG-AAF and dG-AAF/EdU were processed efficiently by NER, but the EdU residue by itself was not (Figure 8). Since EdU residue does not trigger or interfere with the NER reaction, it is well suited for the proposed labeling strategy. In summary, developing these new fluorescent substrates will enable studies that enhance the understanding of the NER pathway by enabling the visualization of various steps of the NER reaction, and may find applications in other laboratories to study DNA repair pathways.
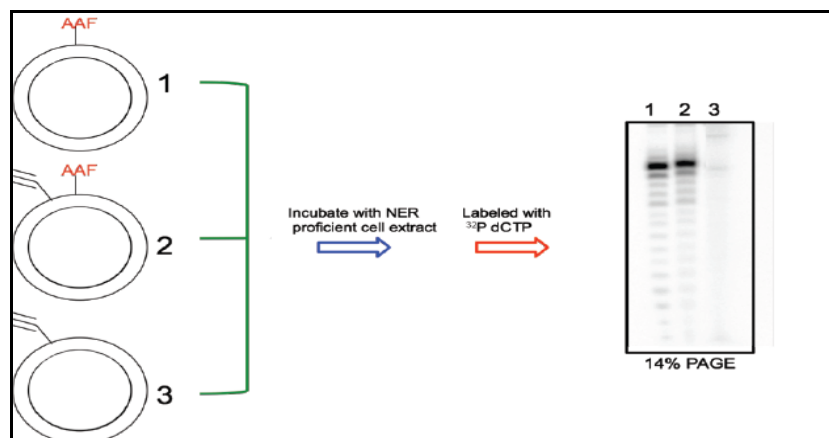

Figure 8: An in-vitro NER assay with different substrates. (Data excerpted from a former member, Jung-Eun Yeo's PhD dissertation [36]) Plasmids containing a lesion, dG-AAF (1), dG-AAF and EdU residue (2) or only presence of EdU residue (3), respectively was incubated with HeLa cell extract. The excised products were analyzed and detected via post-labeling method as describe in figure 3b.

Chapter 2

Result and Discussions:

2.1 Development of an *in-vitro* NER assays using a fluorescent-labeled NER substrate.

As described in figure 4, the procedure for preparing fluorescent NER substrates via pre-labeling method include the purification of oligonucleotides containing the modified base, dG-AABP-K, and its coupling with commercially available hydroxylamine fluorescent dye via oxime formation prior to its incorporation into the plasmid containing a fluorophore in the damaged residue. This plasmid will be incubated in a HeLa cell extract, and the excised NER fragments will be monitored directly by fluorescence detection.

A former group member, Jerome Gualbert synthesized the phosphoramidite containing the dG-AABP analog, and incorporated it into oligonucleotides using ultra mild solid phase DNA synthesis. The sequence of the 12mer oligonucleotide used to optimize the coupling reaction with the oxime was 5'-TAC CGG C**X**C CAC-3', where **X** is the modified base. The oligonucleotide was cleaved from the solid support and protecting groups were removed using an "ultra-mild" deprotection procedure developed by our laboratory, ensuring that the base labile acetyl group at N-8 position would remain intact. The deprotected product was purified using reverse-phase high pressure liquid chromatography (RP-HPLC) on a C18 column using a gradient of acetonitrile in 0.1 M TEAA buffer (Figure 9). The purity of the oligonucleotide was determined by running the purified product on a denaturing polyacrylamide gel electrophoresis (PAGE) and analyzed the desired product by electrospray ionization mass spectrometry (ESI-MS) method (Supplementary Figure 1). The DMTr-group at the 5'-OH position of the oligonucleotide was removed under weakly acidic conditions with 80% acetic acid. The

15

detritylated product was repurified by RP-HPLC and validated by ESI-MS (Supplementary Figure 2) (Figure 10).
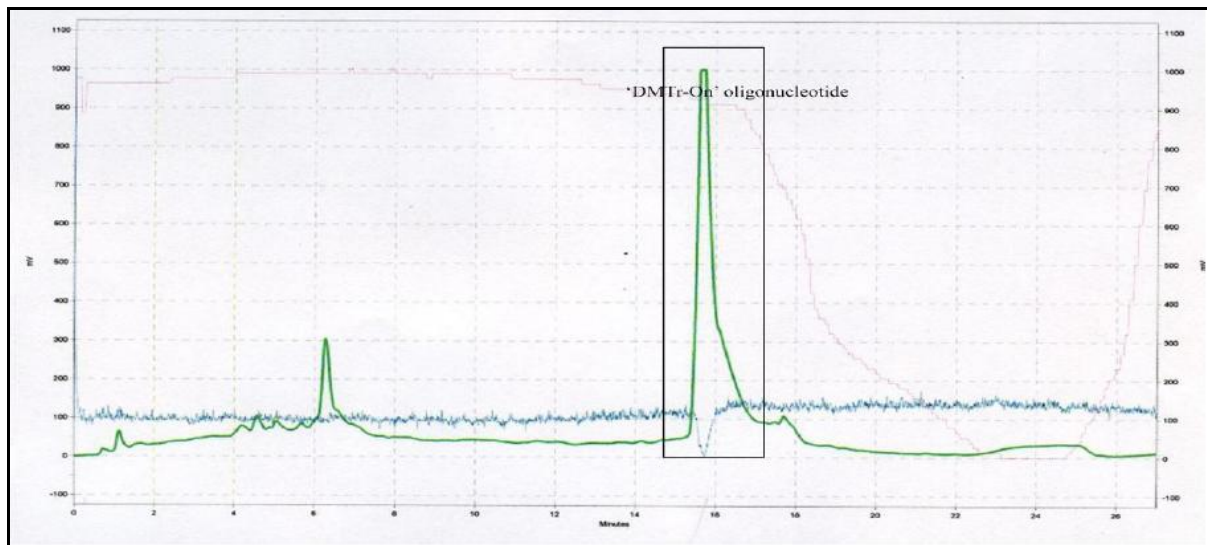

Figure 9: Purification of the 'DMTr-On' oligonucleotide after MeOH/iPr₂NH deprotection. The oligonucleotide was separated from impurities using a HPLC gradient of : linear 5-30% B over 16 min, linear 30-95% B until 22 min, isocratic 95% until 24 min, linear 95-5% B until 27 min; buffer A: 0.1 M TEAA (pH 7); buffer B: CH₃CN. The peak of the 'DMTr-On' oligonucleotide eluted between 15 and 16 minutes.
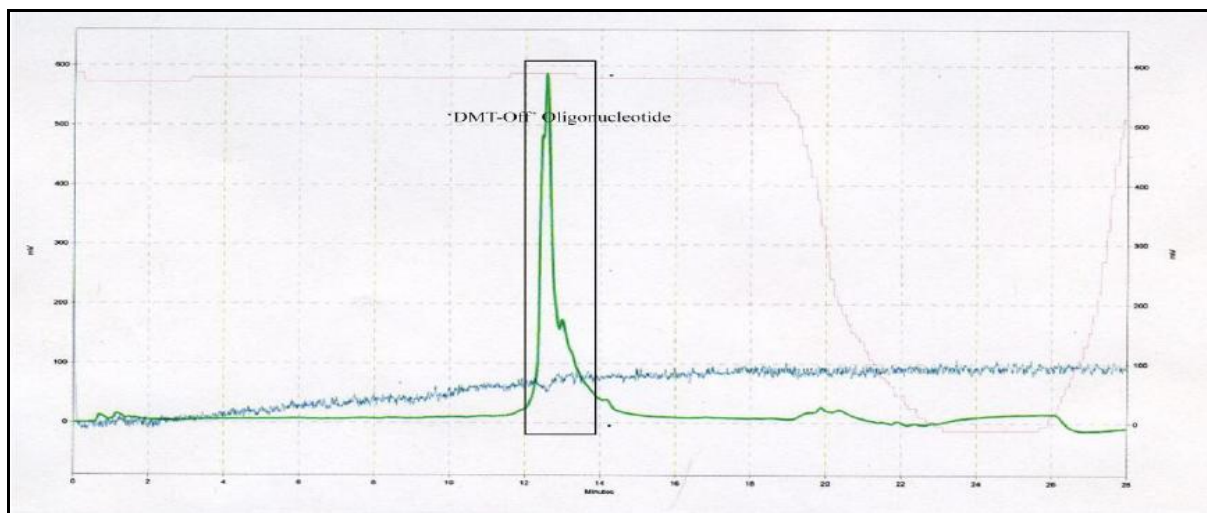

Figure 10: Purification of the 'DMTr-Off' oligonucleotide after acetic acid treatment. The oligonucleotide was purified by HPLC over a C18 column using a gradient of linear 5-20% B over 18 min, linear 20-95% B until 22 min, isocratic 95% until 26 min, linear 95-5% B until 28 min; buffer A: 0.1 M TEAA (pH 7); buffer B: CH₃CN. The peak of the 'DMTr-Off' oligonucleotide eluted between 12 and 13 minutes.

The purified oligonucleotide containing a modified base was incubated with Alexa 488 hydroxylamine in the presence of the reducing agent, sodium cyanoborohydride (Figure 11). The coupling product was analyzed by denaturing PAGE and by RP-HPLC (Figure 12).
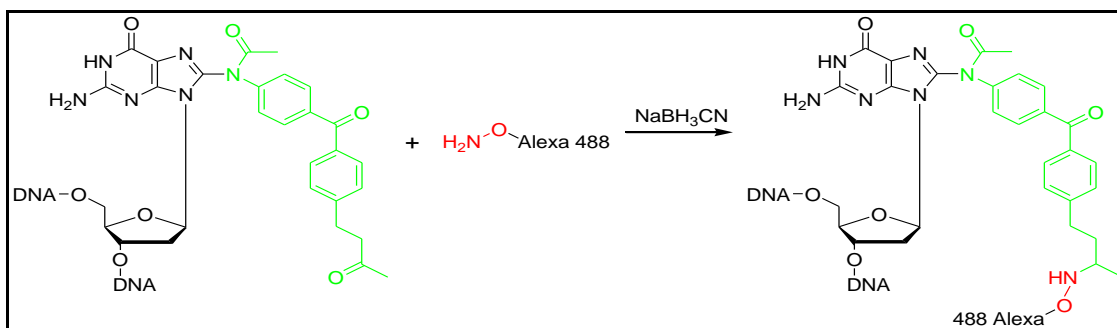

Figure 11: Coupling dG-AABP analog with Alexa 488 hydroxylamine yielding fluorescent substrate. Reaction condition: 20nmol equiv. Alexa 488 hydroxylamine dye, 0.4 M NaOAc, pH 4.1, 20nmol equiv. NaBH$_3$CN, 30°C, overnight
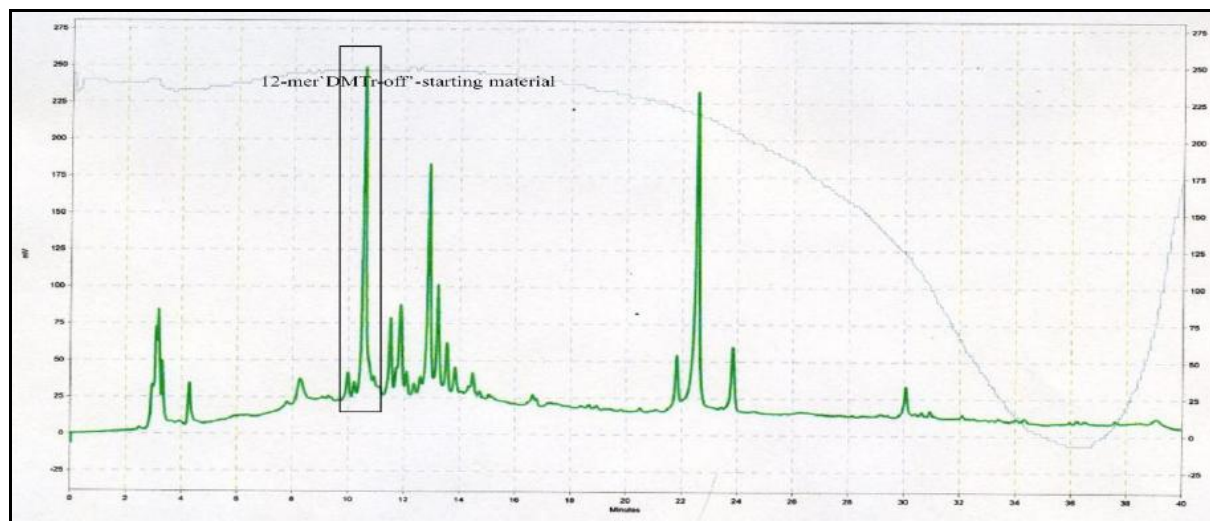

Figure 12: HPLC trace of the coupling reaction of the ketone-containing oligonucleotide with the hydroxylamine-coupled Alexa dye. The starting material and products were separated using on C18 column by HPLC with a gradient of linear 5-30% B over 20 min, linear 30-95% B until 28 min, isocratic 95% until 33 min, linear 95-5% B until 34 min; buffer A: 0.1 M TEAA (pH 7); buffer B: CH$_3$CN. The staring material eluted at 11 minutes. The peaks eluting at 12, 13, and 23 minutes were collected for ESI-MS analysis.

The coupling products have higher molecule weights and longer retention times than the starting material on a C18 column due to the change in polarity after the incorporation of the fluorescent tag. Peaks representing possible coupling products were purified by using RP-HPLC and

characterized by ESI-MS but the mass spectra data did not reflected the total molecular weights of corresponding oligonucleotide coupled to the fluorescent dye (Figure 12). Several optimization experiments were conducted with the hope to obtain higher coupling yields, for example, variation of the pH and temperature of the reaction, and altering the molar ratio of oligonucleotide and the dye. However, changes to the reaction conditions yielded results similar to the previous ones, and no new coupling products could be characterized. It has been reported that the buffer composition and pH range can influence the yield of the coupling reaction between a ketone of an oligonucleotide and a fluorescent dye [37]. As a result, the coupling reaction was tested with phosphate and sodium acetate buffers and analyzed on a denaturing PAGE (Figure 13).
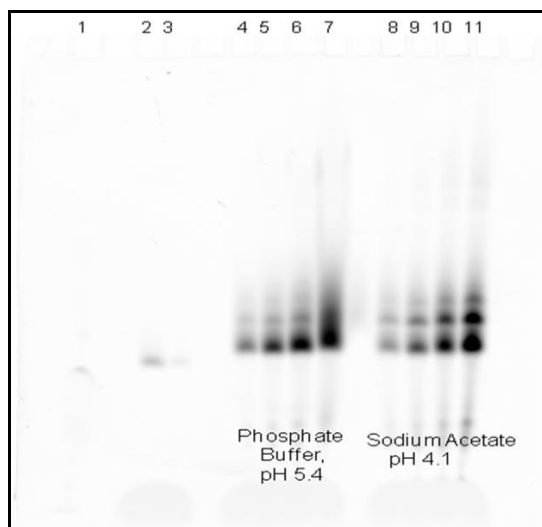

Figure 13: Coupling reaction between the dG-AABP-K-containing oligonucleotide and the Alexa hydroxylamine fluorescent dye using phosphate (pH 5.4) and sodium acetate buffer (pH 4.1). The purified oligonucleotide was incubated as described in Figure 11, and loaded on a 20% PAGE. Lane 1: Formamide loading blue dye, Lane 2: 50 fmol of Alexa dye, Lane 3: 1 pmol of starting material, (Lane 4, 8: 200fmol, Lane 5, 9: 500fmol, Lane 6, 10: 1 pmol, Lane 7, 11: 2 pmol) of reaction in phosphate and sodium acetate buffers, respectively.

As shown in Figure 13, significant shifts in the bands were observed for the coupling reactions in either phosphate or sodium acetate buffer as compared to the Alexa 488 fluorescent dye (Lane 2). However, since the starting material was not visible, it was difficult to directly

18

compare between the starting material and the product, 12-mer modified oligonucleotide (Figure 13: Lane 3). Therefore, the starting materials and coupling products were visualized by labeling the oligonucleotides with γ-[^{32}P]-ATP and of polynucleotide kinase (PNK) at the 5' end, and analyzed on the 14% sequencing gel (Figure 14).
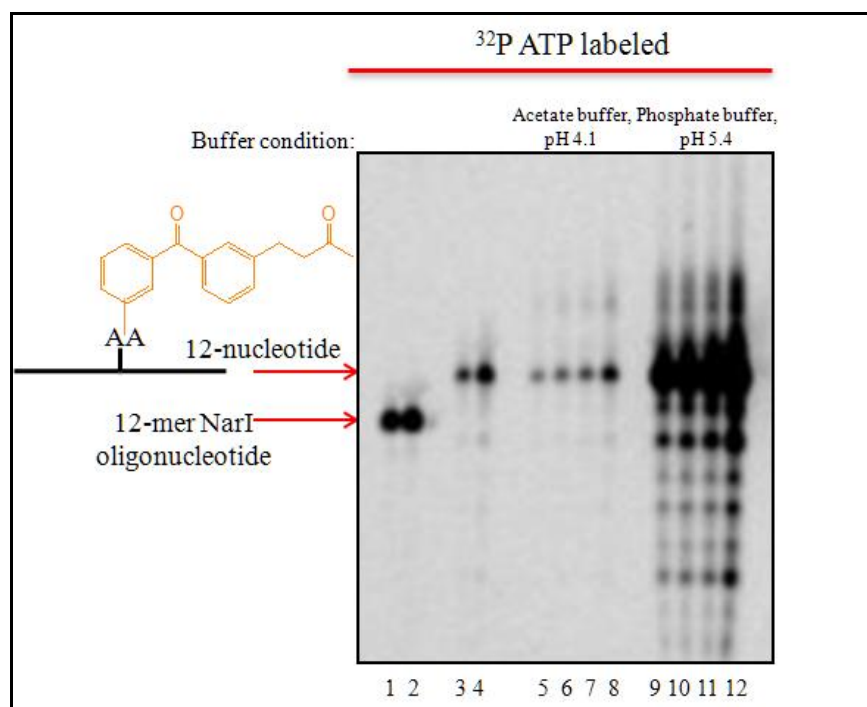

Figure 14: The coupling reactions, starting material and a reference 12-mer oligonucleotide were labeled with ^{32}P-ATP, and analyzed on a 14% sequencing gel. (Lanes 1,2: 10, 20 fmol of the 12-mer oligonucleotide, Lanes 3,4: 10, 20 fmol of starting material, (Lanes 5,9: 20 fmol, Lanes 6, 10: 40 fmol, Lanes 7, 11: 60 fmol, Lanes 8,12: 80 fmol,) of the reaction mixtures in phosphate and sodium acetate buffers respectively.

Figure 14 shows that no significant amount of new coupling products were formed as most of the radioactive signals came from the starting material, indicating that the coupling yield between the modified oligonucleotide and Alexa 488-hydroxylamine dye is relatively low. One of the possible reasons for the low yield of the product could be the relatively low reactivity of the ketone in coupling reaction with the hydroxylamine group of the fluorescent dye, although similar reaction have been successful in previous reports [37]. An alternative would be the use of an aldehyde instead of the ketone, which is more susceptible to nucleophilic attack from a free

19

amine or hydroxylamine [38,39,40]. To test this notion, we used an 11-mer oligonucleotide synthesized by our group member, Shivam Mukherjee, containing the modified base with an aldehyde for the generation of DNA interstrand crosslinks (ICLs) [41,42]. This oligonucleotide contained a 2,3-hydroxypropanyl group at C7 of one of the deazaguanine residues that was oxidized to the aldehyde using sodium periodate (Figure 15), and then incubated with the Alexa 488 hydroxylamine fluorescent dye under coupling condition used for the ketone group.
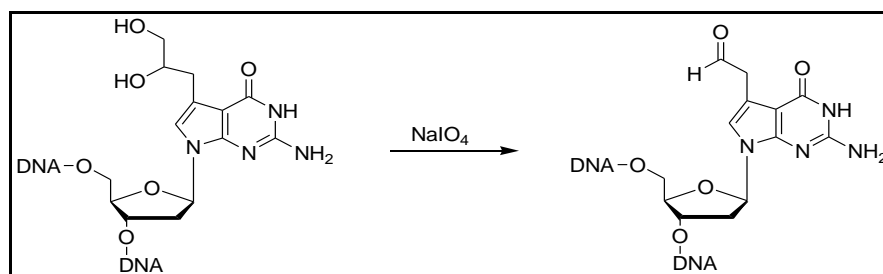

Figure 15: A scheme of the modified base, diol is oxidized to aldehyde in the presence of sodium periodate.
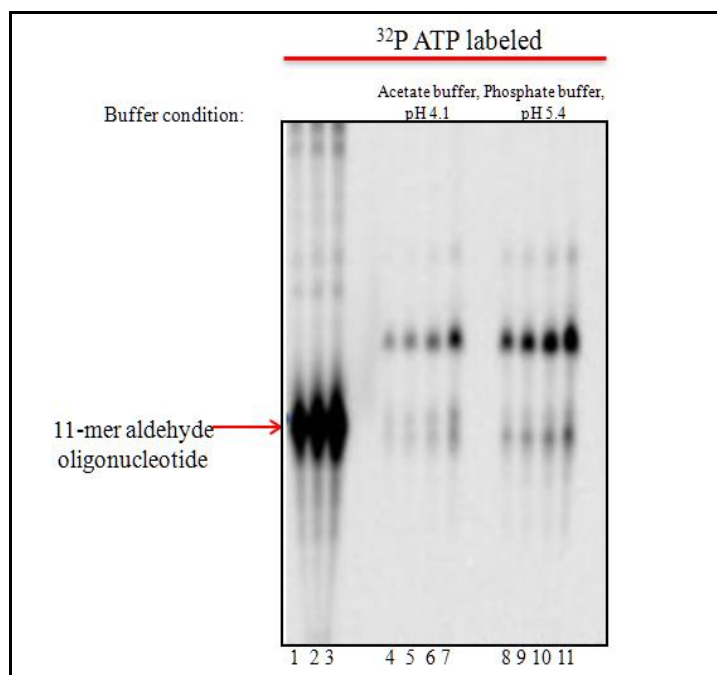

Figure 16: The 11-mer oligonucleotide containing aldehyde functional group was coupled to a hydroxylamine fluorescent dye, and the reaction products and starting material were labeled with ^{32}P-ATP, and loaded on 14% sequencing gel. Lanes 1, 2, 3: 10, 20, 40 fmol of the 11-mer oligonucleotide containing an aldehyde functional group, and Lanes 4, 8: 20 fmol, Lanes 5, 9: 40 fmol, Lanes 6, 10: 60 fmol, Lanes 7, 11: 80 fmol were reaction samples in the buffer used as indicated.

Analysis of the reaction on a 14% sequencing gel (Figure 16) revealed the formation of new bands with lower mobility than the starting material. The bands for the remaining uncoupled starting material were quite weak, indicating that this coupling reaction was very efficient. To isolate the coupling products, the reaction mixture was subjected to the RP-HPLC using a gradient of acetonitrile in 0.1 M TEAA buffer (Figure 17). The HPLC trace revealed that there was a dramatic decrease in the intensity of the peak of the starting material (Compared to HPLC of starting material in Supplementary Figure 3). Two major new peaks with the longer retention time were observed that could be the possible coupling products. These peaks were collected and characterized by the MALDI-TOF-MS. The peak that eluted at 13.6 minutes corresponded to the desired product (MW: 4064, Supplementary Figure 4). These results suggest that the aldehyde in
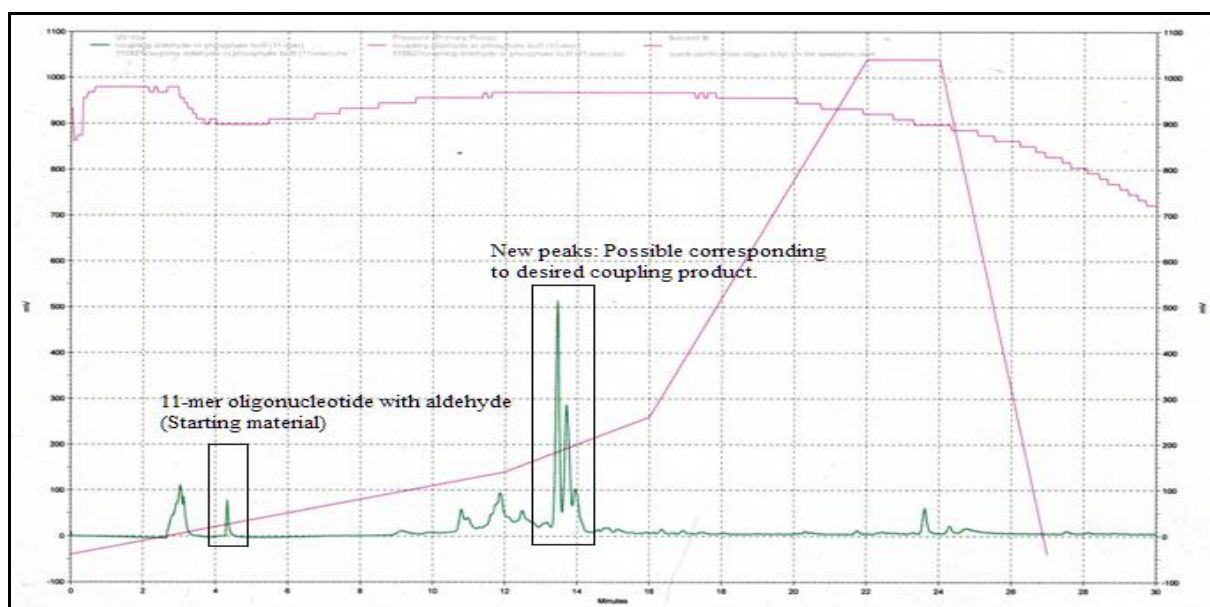

Figure 17: Purification of the coupling product using RP-HPLC. The products and starting materials were separated using HPLC on a C18 column using a gradient of linear 5-30% B over 20 min, linear 30-95% B until 28 min, isocratic 95% until 33 min, linear 95-5% B until 34 min; buffer A: 0.1 M TEAA (pH 7); buffer B: CH$_3$CN. The peak of the 11-mer oligonucleotide containing aldehyde functional group (staring material) was eluted at 4.2 minutes. The peaks eluting at 13.6, 13.8, and 14 minutes, representing possible products were collected for MALDI-MS analysis.

21

DNA readily couples with a hydroxylamine-coupled fluorescent dye, confirming that there is a difference in reactivity between the ketone and aldehyde functional groups. It may therefore be advantageous to have an aldehyde functional group attached to the benzophenone instead of a ketone for coupling with the Alexa fluorescent dye. Future work will therefore involve the design of a novel synthetic route to synthesize the dG-AABP nucleoside containing a protected aldehyde group. This will require a protection group strategy to prevent any side-reactions from occurring due to the enhanced reactivity of the aldehyde group compared to the ketone. Another alternative strategy to improve the coupling yield would be to synthesize dG-AABP derivatized with an alkyne linker to introduce a fluorescent dye via click chemistry.

2.2 Development of a NER in vitro assay using fluorescent labeling by click chemistry.

Our second approach toward the preparation of new fluorescent NER substrates involved the incorporation of an oligonucleotide containing an alkyne group at a thymine residue in the vicinity of a lesion, in our case a dG-AAF residue, into the plasmid. Following incubation with a NER proficient cell extract, the excised NER products will be fluorescently labeled using a click reaction with an azide-conjugated dye, and visualized by fluorescence detection using the Typhoon imaging system.

A former group member, Jung-Eun Yeo synthesized oligonucleotides containing either 5-ethynyl-dU (EdU) or 5-octadiynyl-dU (OdU) residues that were used to label the DNA with azide-fluorescent dye via click chemistry (Figure 18) [36,43]. These studies revealed that 5-octadiynyl-dU (OdU)-containing oligonucleotides were labeled more efficiently with the azide-conjugated fluorescent dye via click chemistry than those containing 5-ethynyl-dU (EdU). A possible reason for inefficient click reaction of EdU residue may be the compact structure of the
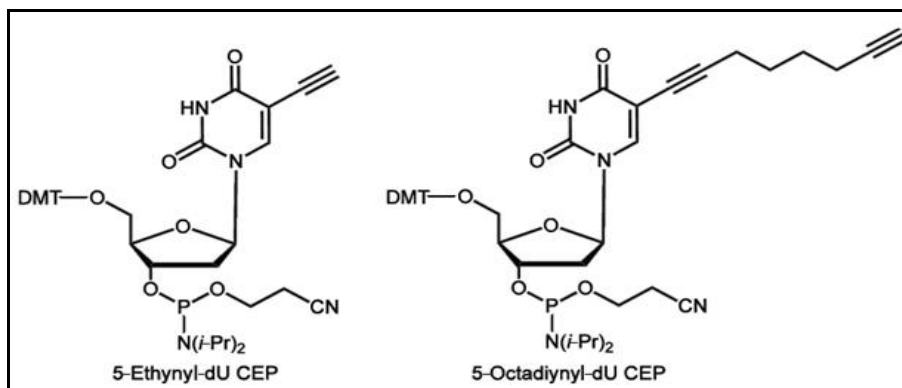
22

Figure 18: Structures of a 5-ethynyl-dU CEP and 5-octadiynyl-dU CEP. DMT: 4, 4-dimethoxytrityl group, CEP:2-cyano-N,N-diisopropylphosphoramidite.

oligonucleotide with a short and rigid alkyne group that restricts the accessibility of the fluorescent dye in the coupling reaction [43]. In contrast, the longer linker of OdU residue has more flexibility enabling a successful tagging of the fluorescent dye using a click reaction [35,43].

In this project, four different sequences of 24-mer oligonucleotides containing an OdU residue with and without the lesion, dG-AAF were used to optimize the click reactions (Table 2).

Name	Sequence
24-mer OdU- 1 without AAF	5' – TAG CTA **U**TA CCG GCG CCA CAT GTC – 3'
24-mer OdU- 2 without AAF	5' – **U**AG CTA TTA CCG GCG CCA CAT GTC – 3'
24-mer OdU- 3 with AAF	5' – TAG CTA **U**TA CCG GC**X** CCA CAT GTC – 3'
24-mer OdU- 4 with AAF	5' – **U**AG CTA TTA CCG GC**X** CCA CAT GTC – 3'

Table 2 : Sequences of the oligonucleotides used for optimization of the click reactions. The oligonucleotides were synthesized using expedite DNA synthesizer, where X is modified base, dG-AAF and U is Octadiynyl-dU.

All the oligonucleotides were synthesized using "ultra-mild" protecting groups and solid support [44], deprotected from solid support using the "ultra-mild" (if containing dG-AAF and OdU) or standard (if containing OdU only) deprotection conditions, and purified by RP-HPLC (Supplementary Figure 5). The identity of the oligonucleotides was confirmed by ESI-MS. The DMTr-group at the 5'-OH position of the oligonucleotide was removed under weakly acidic conditions using 80% acetic acid. The detritylated product was purified by RP-HPLC (Supplementary Figure 6) and validated by ESI-MS (Supplementary Figures 7, 8). The coupling of oligonucleotides containing the 5-OdU residue to azide-conjugated dyes was then tested using a number of different conditions for the click reaction. The first set of conditions involved the use of a copper (I)-chelating ligand, tris (benzyltriazolylmethyl) amine (TBTA) to stabilize the oxidation state of the Cu(I) and to accelerate the rate of the reaction [35,45]. OdU-containing oligonucleotides were incubated with CuBr and TBTA (in a ratio of) 1:2 together with the azide-conjugated Alexa dye [45]. The reactions were quenched by the addition of EDTA, and reactions were analyzed on a 20% denaturing PAGE (Figure 19). Analysis of the reaction by fluorescence detection revealed the formation of new bands for OdU-containing oligonucleotides, with and without damage dG-AAF residues (Figure 19: Lanes 3-6). The bands of the new products have the same mobility as a control band observed in lane 2 (Figure 19) [36], indicating that this new click reaction was successful. However, a drawback of this condition is the long reaction time of 10-12 hours. We therefore examined alternative reaction conditions for more effective labeling with a shorter reaction time. We used combination of the $CuSO_4$, the ligand Tris-(3-hydroxypropyl-triazolylmethyl)-amine (THPTA), sodium ascorbate and aminoguanidine. The function of sodium ascorbate was to reduce the copper (II) *in situ* to the copper (I) oxidation state. In addition, THPTA was used to capture reductive reactive oxygen species produced by
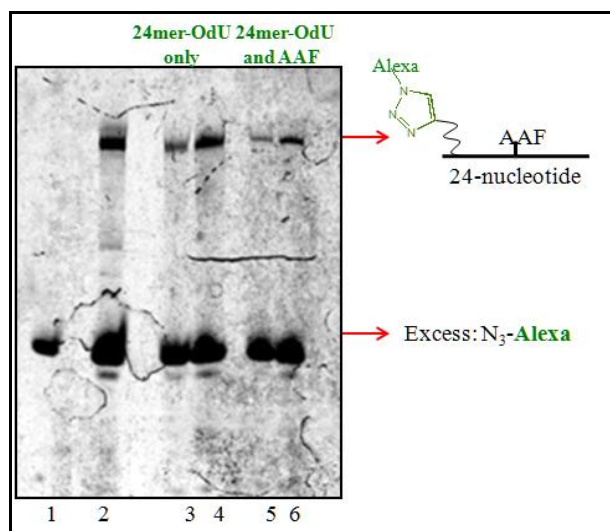
Figure 19: Click reaction using CuBr and TBTA condition. The reaction subjected to a click reaction with CuBr and TBTA, and analyzed on a 20% denaturing PAGE. Lane 1: 100fmol of azide-Alexa dye, Lane 2: 100fmol of 24-mer-labeled-Alexa, Lanes 3, 4: 50, 100 fmol of OdU-containing oligonucleotide, Lanes 5, 6: 50, 100 fmol of OdU and dG-AAF containing oligonucleotide.

the reduction of copper by ascorbate and aminoguanidine was added to neutralize byproducts of ascorbate oxidation [46]. The OdU-containing oligonucleotides were incubated under these reaction conditions with the azide-conjugated dye, and reactions analyzed by 20% denaturing PAGE (Figure 20).
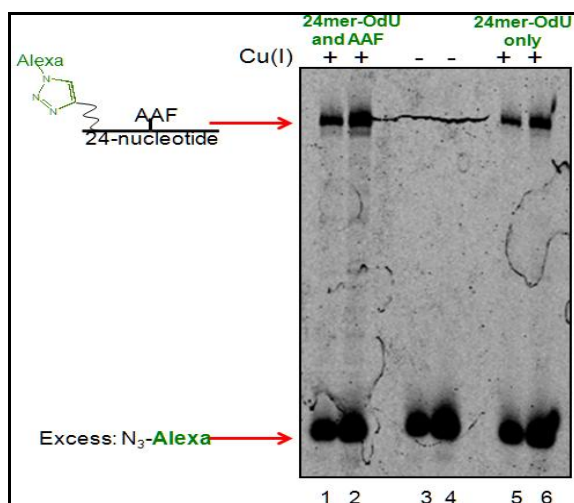

Figure 20: Click reaction using CuSO$_4$ and THPTA condition. The reaction subjected to a click reaction with CuSO$_4$, THPTA, sodium ascorbate and aminoguanidine and analyzed on a 20% denaturing PAGE. Lanes 1, 2: 20, 50 fmol of 24-mer OdU-4 with CuSO$_4$, Lanes 3, 4: 20, 50 fmol of 24-mer OdU-/without CuSO$_4$, Lanes 5, 6: 20, 50 fmol of 24-mer OdU-2 with CuSO$_4$.

For a negative control, CuSO$_4$ was omitted from the reaction mixture. The appearance of the new bands was observed (Figure 20, Lanes 1-2, 5-6), that was formed only in the presence of Cu(I) (Lanes 3-4) indicating from a successful click reaction. To determine the efficiency of the labeling reaction, the products were 5'-labeled with γ-[^{32}P]-ATP and polynucleotide kinase (PNK), and analyzed on the 14% sequencing gel. The main products formed by click reaction (Figure 21, Lanes 3-6) had a slower mobility than the unreacted starting material, in line with the addition of the fluorescent tag to the oligonucleotide. Weaker bands with the same mobility as the starting material were also observed, indicating the presence of some unreacted oligonucleotide. The click-reaction yield for OdU- only and dG-AAF/OdU-containing oligonucleotides were quantified using Typhoon Imager 9400, and were found to be 77.3% and 88.5%, respectively.
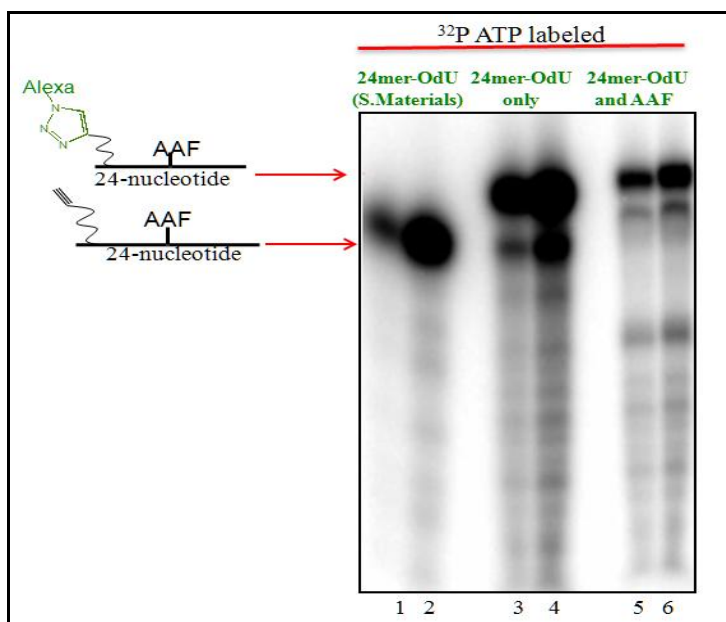

Figure 21: Click reaction substrates and starting oligonucleotide were radiolabeled with ^{32}P ATP. The reaction subjected to click reaction with CuSO$_4$, THPTA, sodium ascorbate and aminoguanidine and analyzed on a 20% denaturing PAGE. Lanes 1, 2: 20, 50 fmol of OdU- 2 (starting material), Lane 3, 4: 20, 50 fmol of OdU-2-click product, Lane 5, 6: 20, 50 fmol of OdU-4-click product.

To further characterize the products, the reaction mixture was applied to a spin column (molecular weight cut off, MWCO= 10 bp) to remove the excess of Alexa dye and copper, and the reaction samples were purified by RP-HPLC (Figures 22 A and B).
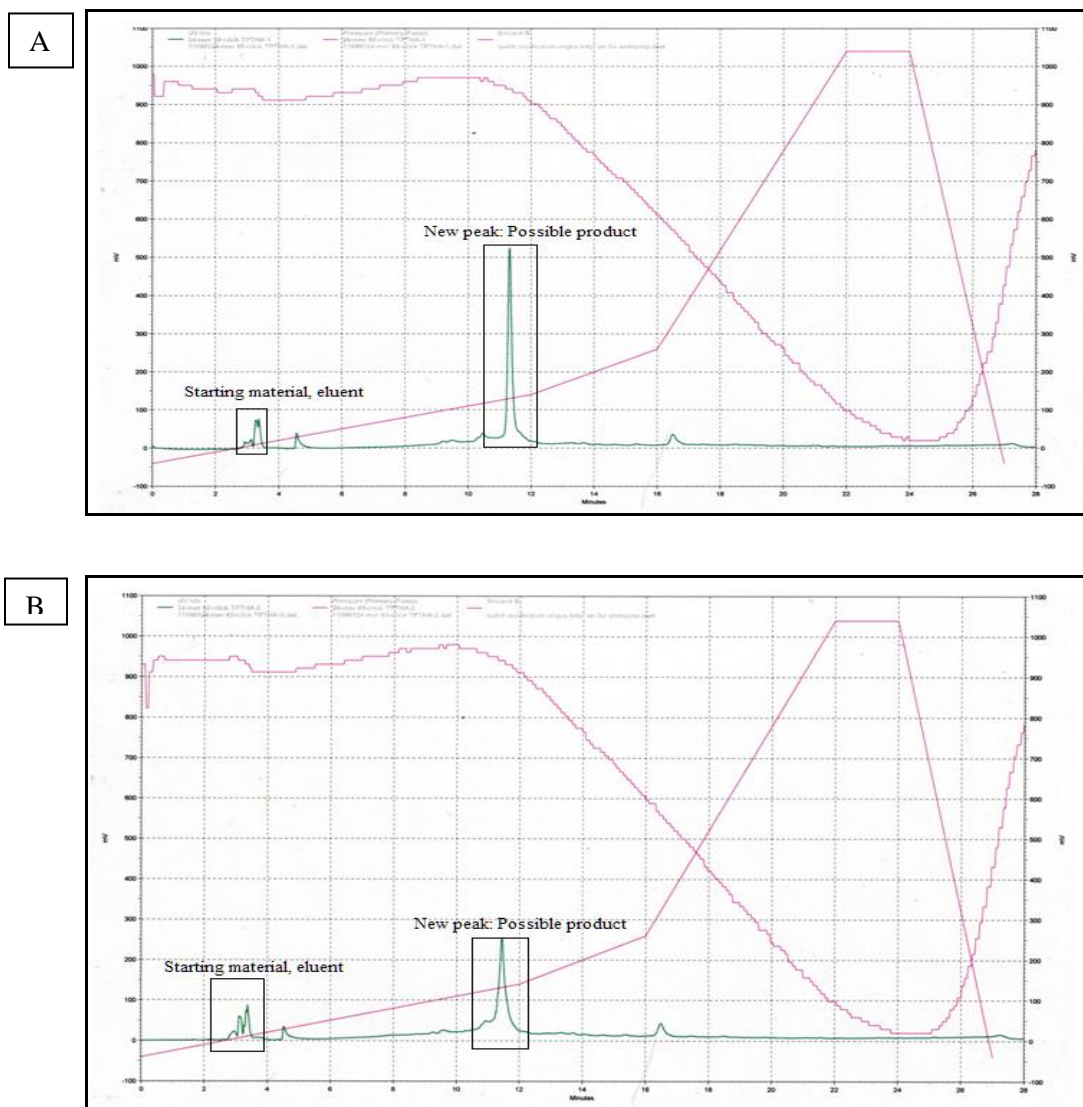

Figure 22: Purification of the coupling products of the click reaction using RP-HPLC. Substrate and product oligonucleotide were separated by RP-HPLC using a gradient of acetonitrile in 0.1M TEAA buffer. **A) Purification for 24-mer-OdU-2-Alexa coupling product:** The peak of the 24-mer oligonucleotide OdU-2 (staring material) eluted at 3.3 minutes. The peak at 11.6 minutes is the possible product and was collected for MALDI-MS analysis. **B) Purification for 24-mer-OdU-4-Alexa coupling product:** The peak of the 24-mer oligonucleotide OdU-4 (staring material) eluted at 3.6 minutes. The possible product peak at 11.8 minutes was collected for MALDI-MS analysis.

New peaks eluting at 11.6 minutes (Figure 22 A) and 11.8 minutes (Figure 22 B) were collected and identified by MALDI-TOF-MS revealing the presence of an oligonucleotide coupled to the Alexa dye which corresponded to the total molecular weight of the oligonucleotide and (MW: 8263 corresponding to 24-mer-AAF-Alexa 488, and MW: 8042 corresponding to 24-mer without AAF-Alexa 488) (see Supplementary Figures 9, 10). This analysis shows that these oligonucleotides were successfully labeled using a click reaction with $CuSO_4$, THPTA, sodium ascorbate and aminoguanidine in one hour.

2.3 Labeling the OdU-containing oligonucleotides excised from plasmid using click chemistry.

The above data shows that we were able to label oligonucleotides containing OdU residues with a fluorescent label via click chemistry. The ultimate goal of this project is to fluorescently label the NER substrates and the excised products from plasmids which obtained after the incubation with the HeLa cell extract. In order to achieve this goal, we started with a simpler experiment where the oligonucleotides containing OdU residues was excised from a plasmid, which was then labeled them with fluorescent dye (Figure 23).
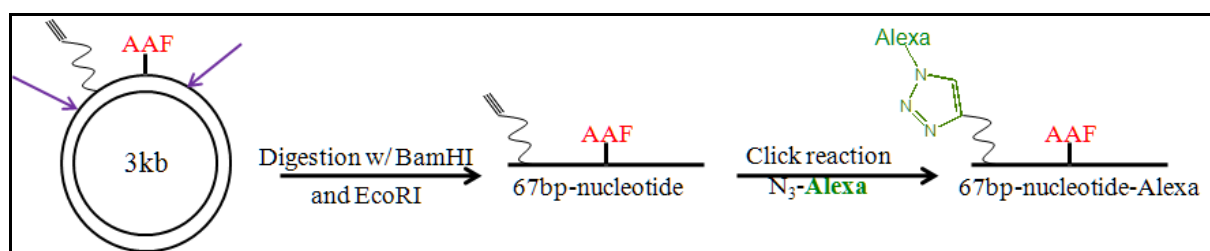

Figure 23: Double digestion of a plasmid containing an OdU residue near a lesion, followed by labeling of the oligonucleotide by a click reaction.

In the experimental setup, a plasmid containing an OdU residue was digested with the restriction enzymes EcoRI and BamHI to yield a 67 bp fragment, which was then reacted with the azide-

dye and a combination of $CuSO_4$, THPTA, sodium ascorbate and aminoguanidine. The reaction

was analyzed by 15% denaturing PAGE (Figure 24). In this labeling reaction, two weak bands

(Bands 1 and 2, Figure 24) were observed below the control-60 mer oligonucleotide that could

not be the expected products. One of the possible explanations for the failure to observe the

desired products could be that an excess of Cu (I) could lead to the degradation of DNA in

particular, since the amount of plasmid used was in fmol scale, while the oligonucleotides were

performed in a nmol scale. Therefore, we conducted two experiments to investigate the origin of
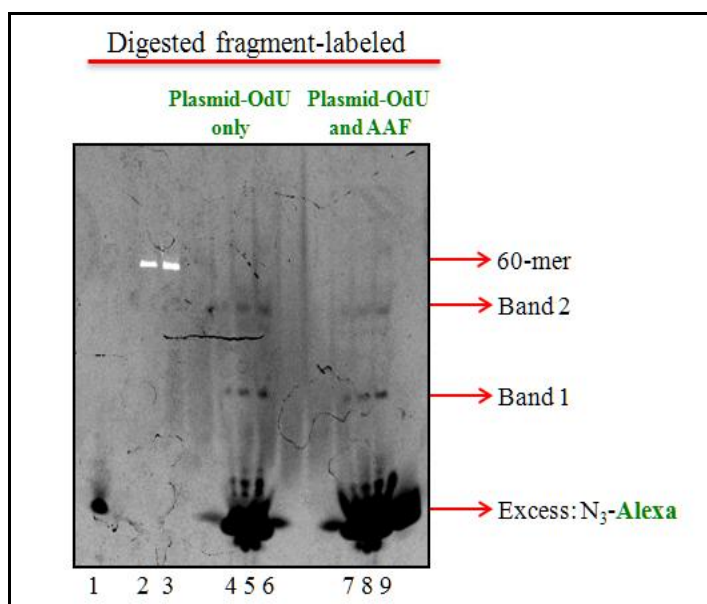

Figure 24: Click reaction after digestion with two restriction enzymes. 100 fmol of the plasmids were incubated with BamHI and EcoRI for 2 hours, and subjected to a click reaction with $CuSO_4$, THPTA, sodium ascorbate and aminoguanidine and analyzed by 15% denaturing PAGE. (Lane 1: 50 fmol of Alexa 488 dye, Lanes 2 and 3: 50 and 100 fmol of a Cy5 labeled 60mer, Lanes 4, 5 and 6: 12.5, 25 and 50 fmol of digested plasmid containing OdU-1, Lanes 7, 8 and 9: 12.5, 25 and 50 fmol of digested plasmid containing OdU-3)

these bands, and to test the effects of the concentration on the click reaction product. In the first

experiment, we varied the concentration of the DNA, while maintaining the concentration of all

other components at the nmol scale (Figure 25-A). In the second experiment, the concentration

of the DNA and all the click components were kept at a fixed molarity ratio, while varying the

overall concentration (Figure 25-B). These studies revealed that the formation of a product band

29

was observed when the amount of DNA was reduced to 100-fmol, with the click reagents at a 1 nmol scale (Figure 25-A, lanes 10 and 11). However, no product was formed when the DNA and click reaction components, at a constant ratio, were reduced to the 100 fmol scale (Figure 25-B, Lanes 9 and 10).
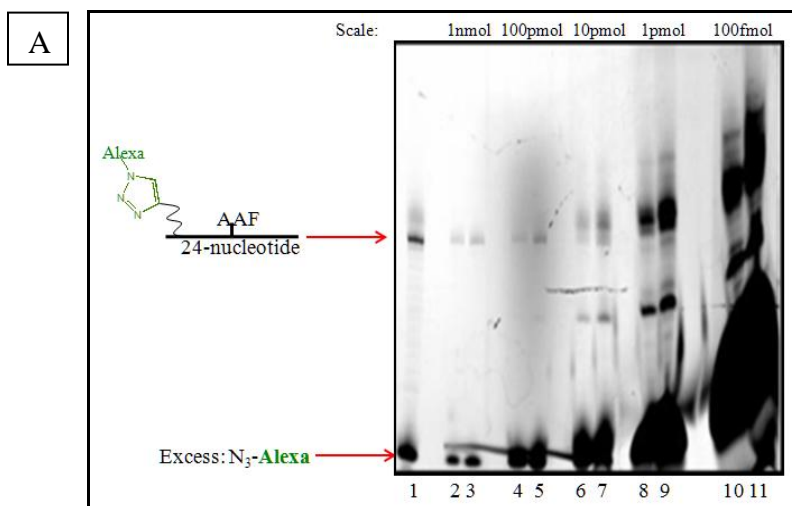

Figure 25-A: The concentration of DNA was varied, while maintaining the concentration of all other components at the nmol scale. The reactions conducted using a click reaction with $CuSO_4$, THPTA, sodium ascorbate and aminoguanidine. Lane 1: 100 fmol of 24-mer-Alexa (control), 50 and 100 fmol of each click reactions were loaded on a 20% denaturing gel, respectively.
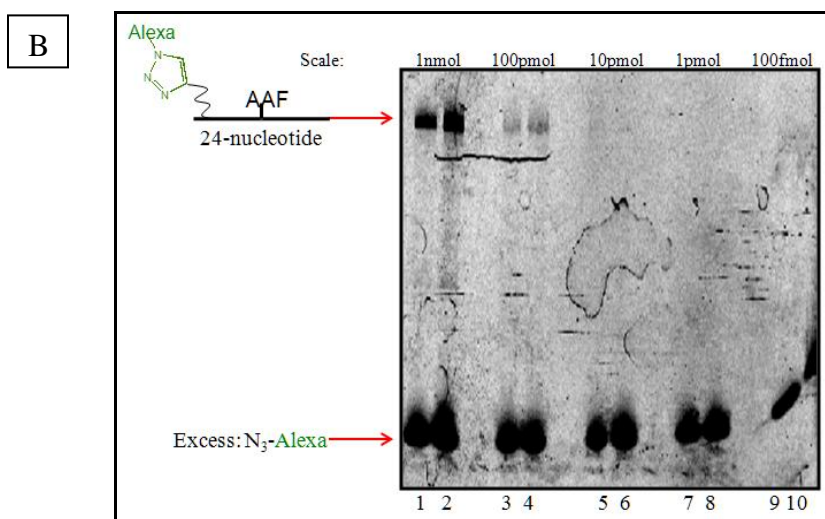

Figure 25-B: The concentrations of DNA and all other components were kept fixed at a fixed molarity ratio, while varying the overall concentration. The reactions conducted using a click reaction with $CuSO_4$, THPTA, sodium ascorbate and aminoguanidine. 50 and 100 fmol of each click reactions were loaded on a 20% denaturing gel, respectively.

The extra band that migrated faster than the desired product was observed when excess of Cu(I) was presence in the reactions (Figure 25A, lanes 6-11). This is expected since excess of hydroxyl radicals can lead to degradation of the DNA. A possible reasons for unsuccessful click reaction with DNA and click components at a lower concentrations may be due to failure of the Cu(I) to interact with the ligand, preventing an effecient click reaction [46]. We therefore varied the molar ratio of the azide-conjugated Alexa dye to DNA (Figure 26-A) and changed the $CuSO_4$ concentration (Figure 26-B). The amount of product formed increased when higher equivalents of the Alexa dye (Figure 26A, lanes 3-10). The highest yield of the product was achieved at 500 equivalent of Alexa dye with respect to DNA. The formation of the lower product band was abolished when the concentration of $CuSO_4$ decreased to 4 μM, although this also impacted the yield of the product.
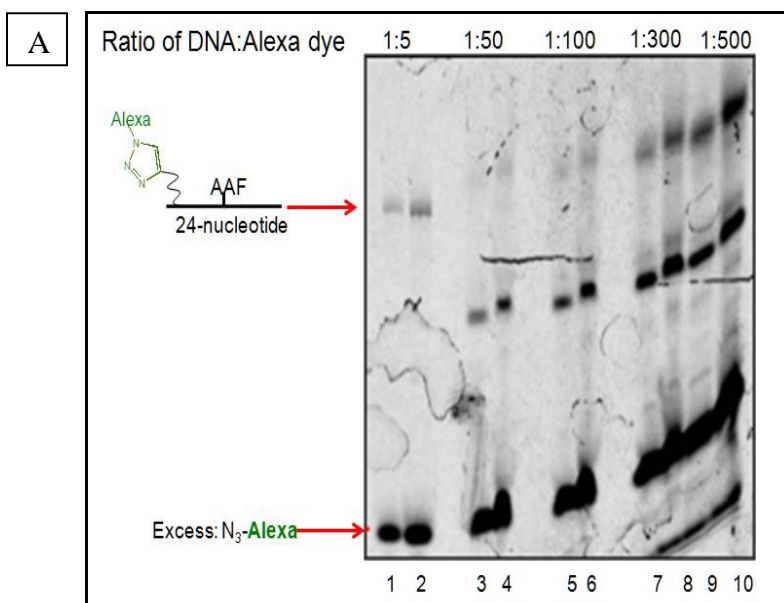

Figure 26-A: Optimization of the click reaction by varying the molar ratio of Alexa 488 dye to DNA. The reactions conducted using a click reaction with $CuSO_4$, THPTA, sodium ascorbate and aminoguanidine. 50 and 100 fmol of each click reactions were loaded on a 20% denaturing gel, respectively.
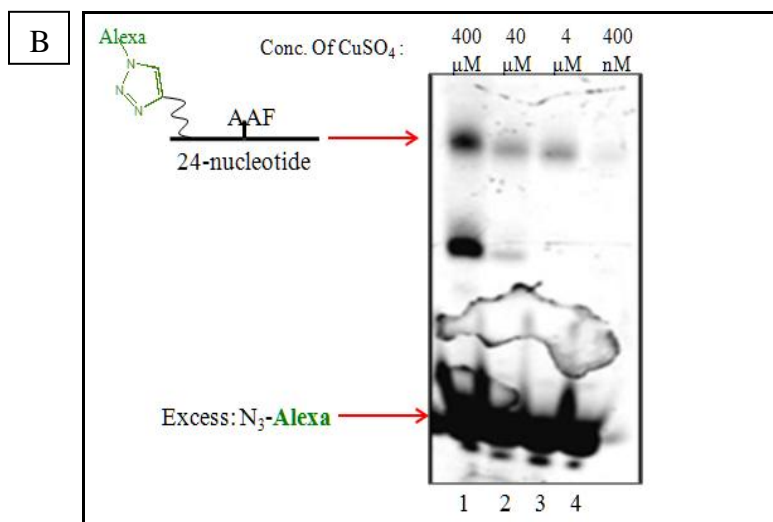
Figure 26-B: Optimization of the click reaction by varying the concentration of CuSO₄. The reactions conducted using a click reaction with CuSO₄, THPTA, sodium ascorbate and aminoguanidine. 50 and 100 fmol of each click reactions were loaded on a 20% denaturing gel, respectively.

We also carried out a time course of click reaction and found that the yield of product increased

from 30 minutes to 2 hours reactions (Figure 27, lanes 3, 5 and 7) but plateaued after that (Figure

27, lanes 7 and 9). These optimized conditions were now applied to fluorescently label the 67bp

Figure 27: Optimized click reactions by varying the incubation time. The reactions conducted using a click reaction with CuSO₄, THPTA, sodium ascorbate and aminoguanidine. 50 and 100 fmol of each click reactions were loaded on a 20% denaturing gel, respectively.
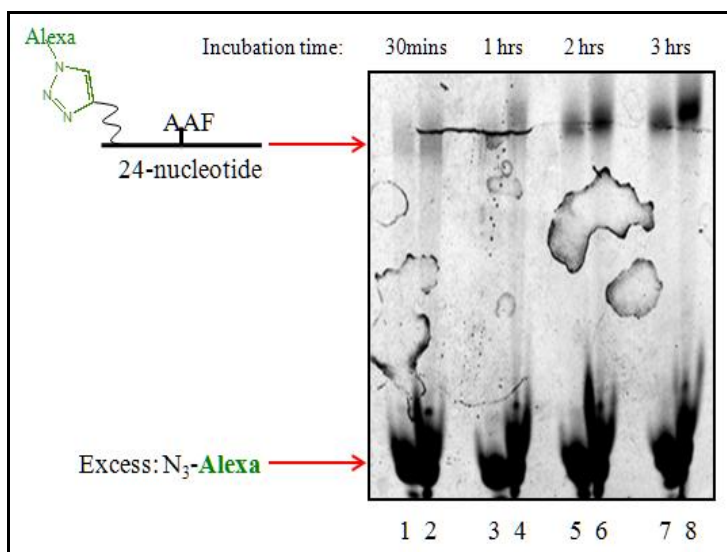
fragments excised from the plasmid (Figure 28). 100 fmol of plasmid was digested with EcoRI and BamHI, and incubated with a 500-fold excess of Alexa 488-azide and CuSO₄/THPTA/ascorbate. Analysis of the reaction by 15% denaturing PAGE revealed the presence a new band that ran as a smear (Figure 28, lanes 4 and 5) that migrated faster than the control 67-mer oligonucleotide. Plausible reasons to explain the unsuccessful labeling reaction could be the presence of the restriction enzymes or the NEB and BSA buffers used in the digestion that may contain elements such as dithiothreitol (DTT) that disfavor the click reaction.
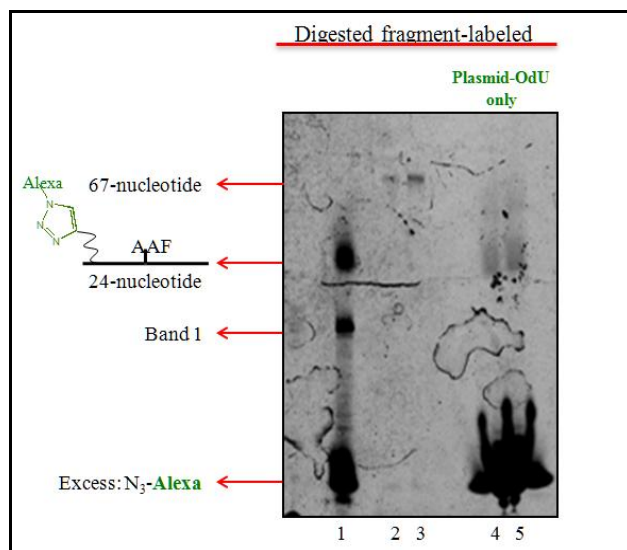

Figure 28: Click reaction after digestion with two restriction enzymes and subjected to an optimized click condition in a molar ratio of 1:500 eq of DNA:Alexa Dye/4μM of CuSO₄/2 hours incubation. All reaction samples were analyzed on a 15% denaturing PAGE. Lane 1: 100 fmol of click reaction (1nmol reaction with excess of Cu(I)), Lanes 2, 3: 20 and 50 fmol of a 67 mer with fluorescently labeled, Lanes 4,5: 50 and 100 fmol of digested plasmid 24-mer OdU-3.

We therefore prepared all buffers by excluding DTT and EDTA. A control enzymatic digestion using these buffers revealed that the restriction enzymes were catalytically active under these conditions (Supporting Figure 11). Additionally, we used clean-up kit (Zymo research, MWCO: 50bp to 10kb) to remove all buffers. We then subjected an OdU-containing oligonucleotide excised from a plasmid under these conditions to a click labeling reaction with Alexa488-azide

(Figure 29). The product bands from this reaction ran as distinct band and were visible even at very low concentrations, 10 and 20 fmol. However, these bands still migrated faster than as with the control 67-mer and the identity of the product remains to be conclusively established.
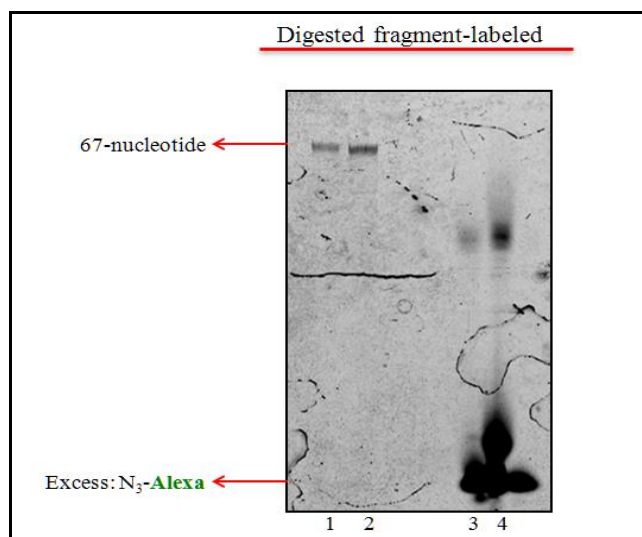

Figure 29: Click reaction after digestion using prepared buffers, optimized click conditions, and enzymatic clean-up kits. All reaction samples were loaded on 15% denaturing PAGE. Lanes 1, 2: 10 and 20 fmol of a 67 mer with fluorescently labeled, Lanes 3, 4: 10 and 20 fmol of digested plasmid 24-mer OdU-3.

2.4 Conclusion

A click coupling reaction between oligonucleotides containing an OdU residue and azide-conjugated Alexa dye was achieved and optimized using two reaction conditions. The desired products were analyzed by denaturing PAGE and 5'-radioalabeling with γ-$[^{32}P]$-ATP, and the identity of the desired products was confirmed by MALDI-TOF mass spectrometry. The click reaction on a fmol scale that will be required for the study of NER reactions was optimized; however, the identity of the desired products from the digestion-click labeling was not yet conclusively established. A possible solution to characterize the observed band would be to perform in a bigger scale, thereby providing sufficient amounts of the substrates for a more thorough analysis. In particular, we will need to confirm that reactive oxygen species generated

by copper(I) do not damage the DNA if it is used at this low concentration. A possible alternative solution could be to use copper-free click chemistry to label the oligonucleotides. Future work is aimed to optimize reaction parameters to enhance the efficiency of the click reaction at a low scale and make the approach practical for routine use in monitoring NER reactions.

Chapter 3

Materials and Methods:

Reagents and equipments:

Chemicals and solvents were purchased from Fluka-Sigma-Aldrich. Reagents for DNA synthesis were purchased from Glen research except 5-ethynyl-2'-deoxyuridine 2-cyanoethyl-*N*, *N*-diisopropylphosphoramidite (CEP) and 5-octadiynyl-2'-deoxyuridine CEP, which were bought from Barry & Associates Company. A 60mer oligonucleotide labeled with Cy5 (Cyanine) were purchased from Integrated DNA Technologies (IDT). HPLC purifications were performed on a JASCO system equipped with a Phenomenex Clarity Oligo-RP Semi-prep column: C18, 5μm, 50×10.00 mm. The C18-SepPak cartridges were purchased from Waters. Alexa fluor 488 hydroxylamine and azide were purchased from invitrogen. 1Kb ladder, polynucleotide kinase (PNK) enzyme, BamHI and EcoRI digestive enzymes were purchased from New England Biolabs (NEB). [α-^{32}P] ATP was purchased from PerkinElmer.

The 24-mer oligonucleotides were analyzed either by Waters micromass platform LCZ or by (MALDI-TOF) (Bruker Daltonics).

<u>"Ultra-mild" deprotection conditions</u>:

The solid support was deprotected with a solution containing 10% (v/v) of diisopropylamine (iPr$_2$NH) in dry methanol at 55°C overnight. The supernatant containing the released oligonucleotide was decanted and concentrated, and then dissolved in 1 mL of 1M triethylamoniumacetate (TEAA) buffered at pH 7. The solution was then passed through a 0.45 μm filter and finally purified by HPLC.

<u>HPLC Purification</u>:

Purification for 'DMTr-On' oligonucleotides, detritylation procedure, and 'DMTr-Off' oligonucleotides:

Reverse-phase HPLC purification: All HPLC elutions were performed at a flow rate of 4mL/min, with the following gradient: linear 5-30% B over 16 min, linear 30-95% B until 22 min, isocratic

95% until 24 min, linear 95-5% B until 27 min; buffer A: 0.1 M TEAA (pH 7); buffer B: CH₃CN. The peak of the 'DMTr-On' oligonucleotide that eluted between 15 and 16 mins was collected, concentrated and treated with 80% acetic acid (300μl) for 40 min at room temperature to remove the 5'-DMTr group. The detritylated solutions were concentrated using SpeedVac, and the oligonucleotide was redissolved in 1 mL of 1M TEAA buffered at pH 7 and repurified on HPLC. The HPLC elutions for 'DMTr-Off' oligonucleotides were perfomed at a flow rate of 4 ml/min, with the following gradient: linear 5-20% B over 18 min, linear 20-95% B until 22 min, isocratic 95% until 26 min, linear 95-5% B until 28 min; buffer A: 0.1 M TEAA (pH 7); buffer B: CH₃CN. The peak of the 'DMTr-Off' oligonucleotide-eluting between 12 and 13 min was collected and concentrated using SpeedVac. The dry samples were further redissolved in 300μL of 1xTE (10mM Tris-HCl, 1mM EDTA), and the concentration was measured using a NanoDrop 1000 (Thermo Scientific). The final product was characterized using ESI or MALDI mass spectrometry.

Coupling conditions:

Coupling of modified oligonucleotide containing ketone with an Alexa 488 fluorescent dye:

Oligonucleotide containing dG-AABP-K (17.7 μL, 2 nmol) was incubated with Alexa 488 hydroxylamine fluorescent dye (2 μL, 10 mM) and sodium cyanoborohydride (1 μL, 500 mM). Then 4 μL of 0.04 M NaOAc (pH 4) and 75.3 μL of a solution of 50/50 of water/acetonitrile were added to the reaction mixture to a total volume of 100 μL. The reaction was incubated at 37°C overnight. Next day the reaction was analyzed by 20% denaturing PAGE.

Different optimization experiments were conducted for the coupling conditions including: variation of either sodium cyanoborohydride concentration (1 mM, 200 μM and 0 mM), or pH of NaOAc buffer (pH 4 and 5), and also varying the molarity of the buffer: 30 mM of phosphate buffer at pH 5.4 and 30 mM of sodium acetate buffer at pH 4.1.

Purification of coupling products of dG-AABP-containing 12-mer oligonucleotide and Alexa 488 hydroxylamine fluorescent dye:

HPLC elutions were performed at a flow rate of 1ml/min, with the following gradient: linear 5-30% B over 20 min, linear 30-95% B until 28 min, isocratic 95% until 33 min, linear 95-5% B until 34 min; buffer A: 0.1 M TEAA (pH 7); buffer B: CH₃CN. The peak of the starting material, "DMTr-off" oligonucleotide, eluted around 11 minutes. Probable coupling products eluted at 12,

13, and 23 minutes respectively. All the samples were collected, dried using SpeedVac and then analyzed by ESI-MS.

Preparation and coupling condition of oligonucleotide containing aldehyde with fluorescent dye:
A solution of the single-stranded oligonucleotide with 2,3-hydroxypropanyl group at C7 of a deazaguanine residue (17 nmol) [42] in 50 µL was incubated with 4 µL of 3.3 mM of $NaIO_4$ and 6 µL of 0.1 M sodium phosphate buffer (pH 5.4). The reaction was kept in dark overnight at 4°C. The next day, excess of $NaIO_4$ was removed by centrifugation through Microcon columns with a 3K cutoff (Milipore). Then the aldehyde-containing oligonucleotide (3.5 µL, 2 nmol) was incubated with Alexa 488 hydroxylamine fluorescent dye (2 µL, 10 mM) and sodium cyanoborohydride (1 µL, 500 mM) in 4 µL of 0.04 M NaOAc buffer (pH 4) and sodium phosphate buffer (pH 5.4). 89.5 µL of a premixed solution of 50/50 of water/acetonitrile was added to the reaction mixture to give a total volume of 100 µL followed by incubation at 37°C overnight.

Purification of aldehyde-containing oligonucleotide coupled to a fluorescent dye:
HPLC elutions were performed at a flow rate of 1mL/min, with the following gradient: linear 5-30% B over 20 min, linear 30-95% B until 28 min, isocratic 95% until 33 min, linear 95-5% B until 34 min; buffer A: 0.1 M TEAA (pH 7); buffer B: CH_3CN. The peak of the 11-mer aldehyde-containing oligonucleotide eluted at 4.2 min and the possible coupling products eluted at 13.6, 13.8 and 14 mins. All these samples were collected and dried using SpeedVac for MALDI-MS analysis.

5´-labeling of oligonucleotide with [32]P:
Oligonucleotide (20 pmol) was incubated at 37°C for 2 hours with 0.5 µL of T4 polynucleotide kinase (T4 PNK) in a 10 µL reaction containing 1 µL of PNK buffer and 0.5 µL of 3.3 µM [γ-^{32}P] ATP. After the reaction was complete, 90 µL of water was added and the sample was loaded on the 1mL syringe of G-25 Sephadex column. 100 µL of loading dye containing formamide was added to the sample, and the mixture heated at 95°C for 5 mins, cooled in ice for 2 mins, and then analyzed on a 14% sequencing gel (0.5x TBE) at 45 W for 3 hours. The reactions products were visualized using a PhosphorImager (Typhoon 9400, Amersham Biosciences).

Click reaction:

Conditions used for click reaction:

1) CuBr and TBTA (Tris-(benzyltriazolylmethyl)amine) condition [45]: Oligonucleotide containing an OdU residue (16.5 µL, 1nmol) was incubated with Alexa 488-azide dye (1 µL, 5.8 mM) in DMSO and the ratio of (3:1) of t-BuOH (3:1) with CuBr (1µL, 10mM) and TBTA (2µL, 10mM) in 20 µL. The reaction was incubated for up to 10 hrs at room temperature with vigorous shaking. Then, EDTA (1µL, 200mM) was added to quench the reaction. Reactions were analyzed by 20% denaturing polyacrylamide gel electrophoresis and visualized using a Typhoon 9400 imager.

2) CuSO$_4$/TPTHA/ascorbate condition [46]: Oligonucleotide containing an OdU residue (16.5 µL, 1 nmol) was dissolved in HEPES solution at pH 7.5 (60.5 µL, 100 mM). Alexa 488-azide dye (1 µL, 5.8 mM) and premixed CuSO$_4$ (1 µL, 20 mM) and THPTA (1 µL, 100 mM) were added to the reaction mixture. This was followed by the addition of aminoguanidine hydrochloride (10 µL 100 mM) and freshly prepared Na ascorbate (10 µL, 100 mM) to a total reaction volume of 100 µL. The reaction was incubated at room temperature with vigorous shaking for 1 hr. Then EDTA (1 µL, 200 mM) was added to quench the reaction. Reactions were analyzed by 20% denaturing polyacrylamide gel electrophoresis and visualized using a Typhoon 9400 imager.

3) Optimized condition: Oligonucleotide containing an OdU residue (1 µL, 100 fmol) was dissolved in HEPES at pH 7.5 (26 µL, 10 µM). Alexa 488-azide dye (1 µL, 5.8 mM) was added followed by the addition of premixed CuSO$_4$ (1 µL, 200µM) and THPTA (1 µL, 1 mM). Aminoguanidine hydrochloride (10 µL, 100mM) and then freshly prepared Na ascorbate (10 µL, 100 mM) were added to the reaction to a total volume of 50 µLThe reaction was incubated at room temperature with vigorous shaking for 2 hours and quenched with EDTA (2 µL, 10 mM). Reactions were analyzed by 20% denaturing polyacrylamide gel electrophoresis and visualized using a Typhoon 9400 imager.

Purification of the click reaction product:

HPLC elutions were performed at a flow rate of 1mL/min, with the following gradient: linear 5-30% B over 20 min, linear 30-95% B until 28 min, isocratic 95% until 33 min, linear 95-5% B until 34 min; buffer A: 0.1 M TEAA (pH 7); buffer B: CH_3CN. The peak of the 24-mer containing OdU-oligonucleotide with and without dG-AAF eluted at 3.3 and 3.6 mins, respectively. The possible coupling product eluted at 11.6 and 11.8 mins. All the samples were collected and dried using SpeedVac for MALDI-MS analysis.

Double digestion of a plasmid containing an OdU residue and labeling of the oligonucleotide using click chemistry:

Buffers: NEB 3:100 mM NaCl, 50 mM Tris-HCl, 10 mM $MgCl_2$, 1 mM dithiothreitol (pH 7.9 at 25°C). BSA storage buffer: 10mg/ml diluted in 20mM KPO_4, 50mM NaCl, 0.1 mM EDTA, 5% glycerol (pH 7.0 at 25°C). Click reaction was carried out in the absence of EDTA and DTT. EDTA binds to copper and DTT interferes with the next step.

i) Digestion protocol: 200 ng (100 fmol) of a plasmid (3 kb) was incubated with 4 units of EcoRI and 4 units of BamHI to give 67 bp in presence of 1 μL of Bovine serum albumin (BSA without DTT) and 1 μL of 10x (NEB#3 without EDTA) in a 10 μL reaction at 37°C for 2 hours. The restriction enzymes were inactivated by heating the reaction to 60°C for 20 minutees. This was followed by the click coupling reaction with Alexa 488-azide as described above. After incubation, the reaction was stopped by the addition of 50 μL of loading buffer containing 80% formamide/10 mM EDTA and heating at 95 °C for 5 min. The samples were run on a 15% denaturing PAGE (0.5x TBE) and visualized by fluorescence (Typhoon 9400, Amersham Biosciences).

Supplementary Data:

1) The purified 'DMTr-ON' 12-mer oligonucleotide containing ketone functional group. Expected molecular weight: 4202.55, Obtained molecular weight: 4200.45
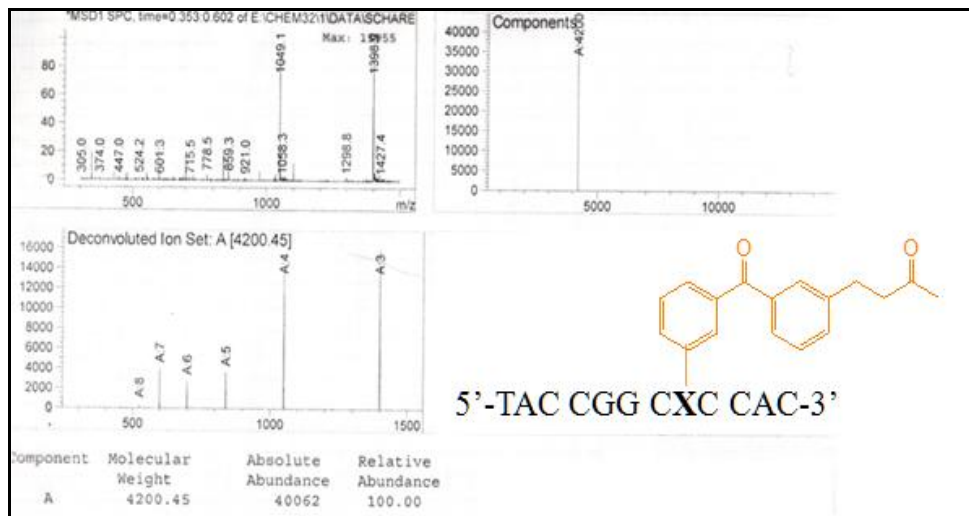

Figure 1: Mass spectrometry (MS) result of 12-mer-AABP-K ('DMTr-on') from ESI, negative mode.

2) The purified DMT "off" 12-mer oligonucleotide containing ketone functional group. Expected molecular weight: 3899.55, Obtained molecular weight: 3898.55
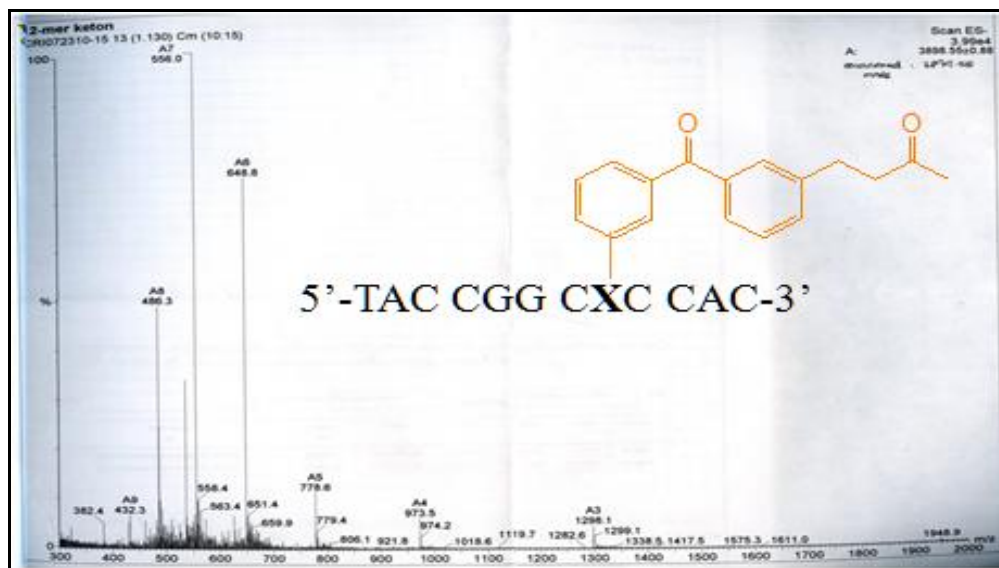

Figure 2: Mass spectrometry (MS) result of 12-mer-AABP-K ('DMTr-off') from ESI, negative mode.

3) HPLC profile for purification of 11-mer oligonucleotide containing aldehyde, starting material:
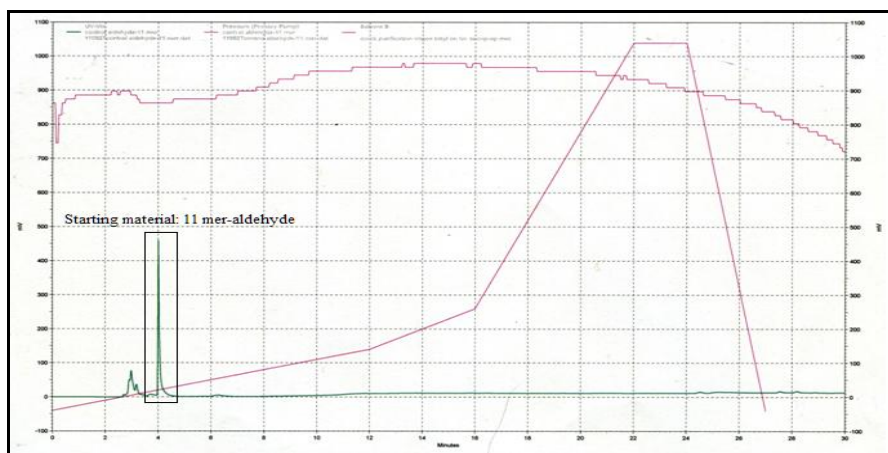

Figure 3: HPLC profile for oligonucleotide containing aldehyde and 'DMT-off': A flow rate of 1ml/min, with the following gradient: linear 5-30% B over 20 min, linear 30-95% B until 28 min, isocratic 95% until 33 min, linear 95-5% B until 34 min; buffer A: 0.1 M TEAA (pH 7); buffer B: CH_3CN. The peak of the 11-mer oligonucleotide containing aldehyde functional group (staring material) was eluted at 4.2 minutes.

4) 11-mer containing aldehyde conjugated with Alexa hydroxylamine 488, Expected molecular weight: 4066.3, Obtained molecular weight: 4064.3
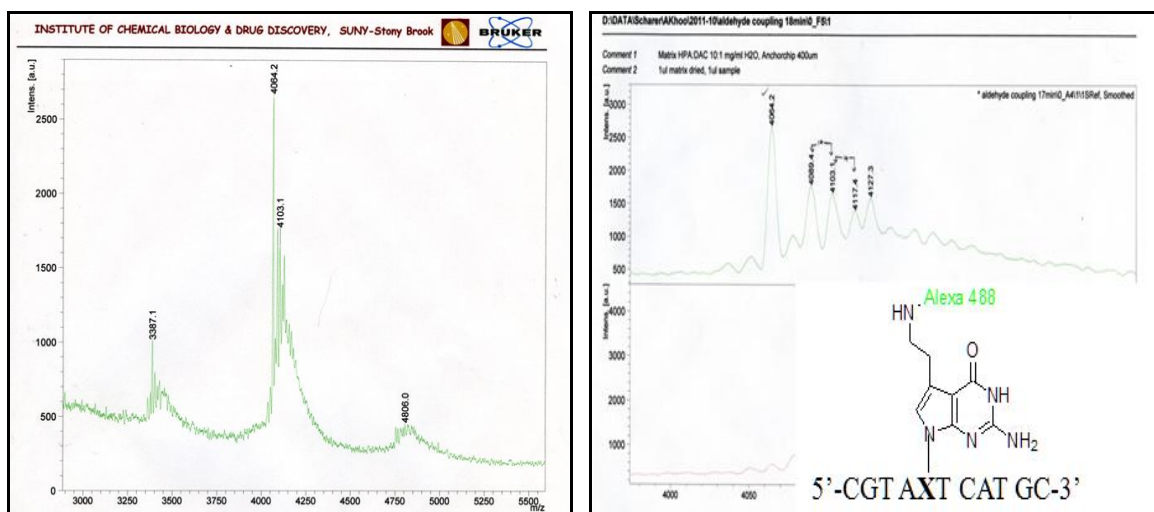

Figure 4: Mass spectra (MALDI) result of 11-mer coupling-Alexa 488-oxime bond, negative mode.

5) HPLC profile for the purification of the 'DMTr-ON' oligonucleotide after MeOH/iPr$_2$NH deprotection.
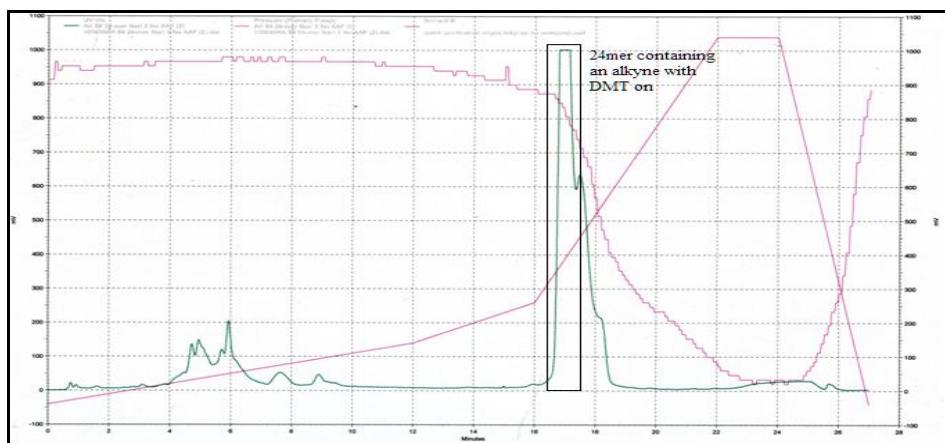

Figure 5: HPLC profile for oligonucleotide containing alkyne and 'DMT-on': A flow rate of 4ml/min, with the following gradient: linear 5-30% B over 16 min, linear 30-95% B until 22 min, isocratic 95% until 24 min, linear 95-5% B until 27 min; buffer A: 0.1 M TEAA (pH 7); buffer B: CH$_3$CN. The peak of the 'DMTr-On' oligonucleotide eluted between 15 and 16 minutes.

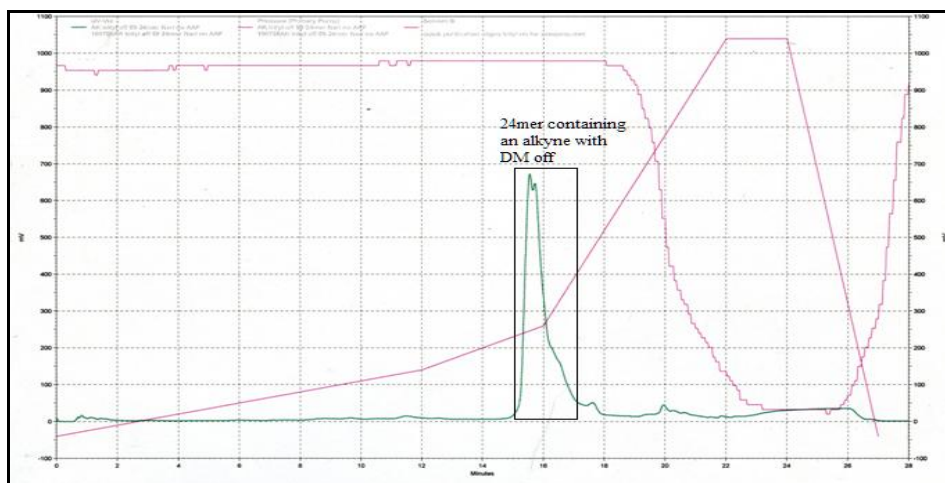6) HPLC profile for the purification of the 'DMTr-Off' oligonucleotide under acetic acid cleavage.

Figure 6: HPLC profile for oligonucleotide containing alkyne and 'DMT-on': A flow rate of 4ml/min, with the following gradient: linear 5-20% B over 18 min, linear 20-95% B until 22 min, isocratic 95% until 26 min, linear 95-5% B until 28 min; buffer A: 0.1 M TEAA (pH 7); buffer B: CH$_3$CN. The peak of the 'DMTr-Off' oligonucleotide eluted between 12 and 13 minutes.

7) 24-mer OdU without AAF: Expected molecular weight: 7379.80; Obtained molecular weight: 7380.36
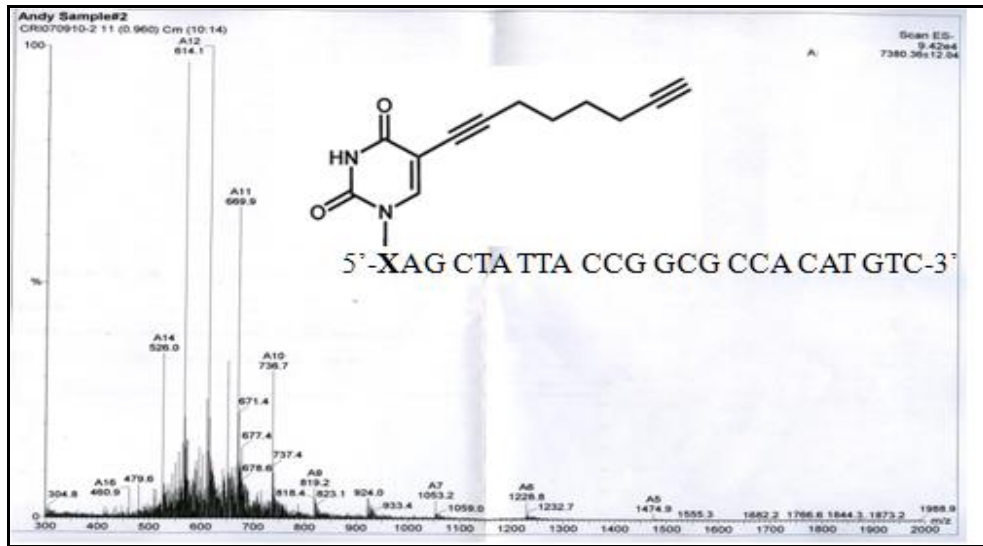

Figure 7: Mass spectrometry (MS) result of 24-mer-without AAF ('DMTr-off') from ESI, negative mode.

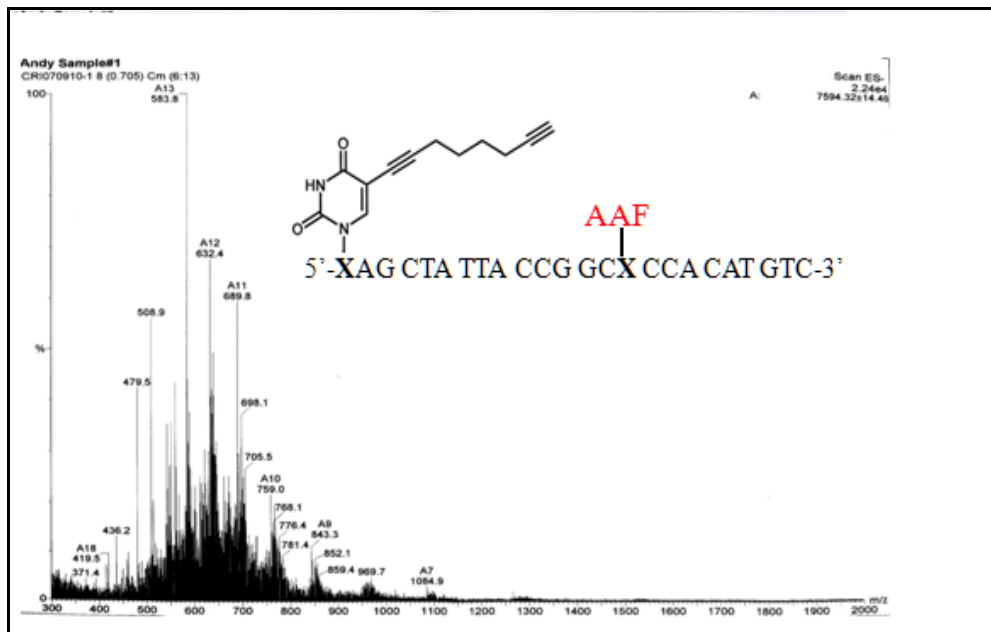8) 24-mer OdU with AAF: Expected molecular weight: 7600.8; Obtained molecular weight: 7594.32

Figure 8: Mass spectrometry (MS) result of 24-mer-with AAF ('DMTr-off') from ESI, negative mode.

9) 24-mer OdU- 1 without AAF conjugated with Alexa 488-clicked, Expected molecular weight: 8044.3, Obtained molecular weight: 8042.3
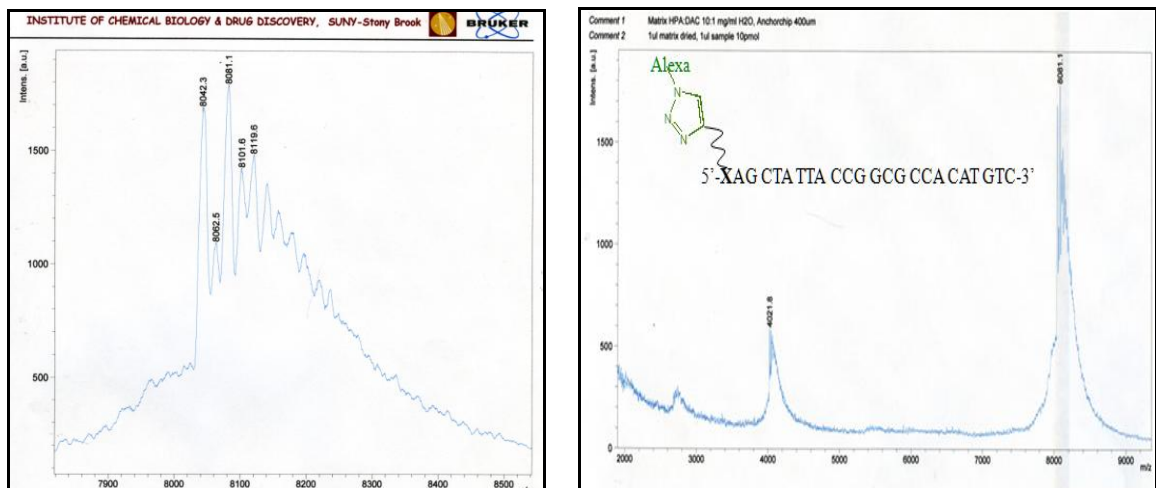

Figure 9: Mass spectrometry (MALDI) result of 24-mer no AAF-Alexa 488 (clicked) from purification.

10) 24-mer OdU- 1 with AAF conjugated with Alexa 488-clicked, Expected molecular weight: 8261.2, Obtained molecular weight: 8263.2
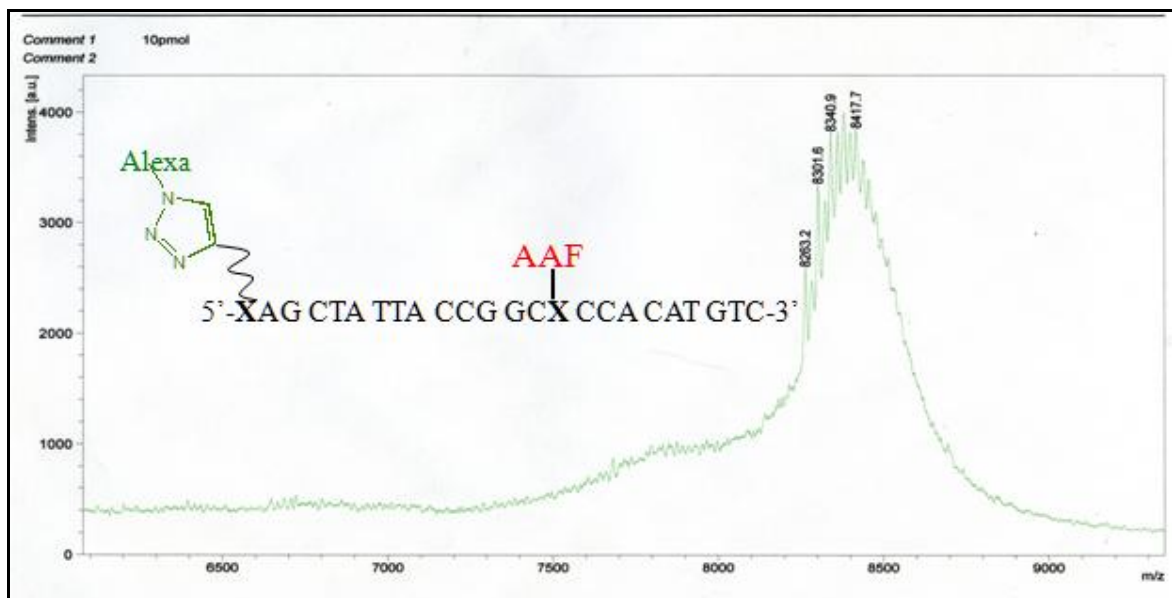
Figure 10: Mass spectrometry (MALDI) result of 24-mer with AAF-Alexa 488 (clicked) from purification.

11) Control enzymatic digestions with the prepared NEB3 and BSA buffers.
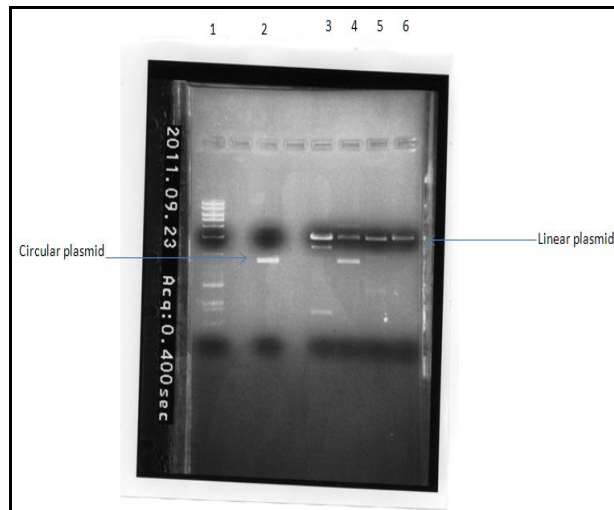
Figure 11: Control enzymatic digestions with buffers lacking EDTA: A plasmid containing an OdU residue was incubated with either EcoRI or BamHI restriction enzymes for 2 hours. The digestion reactions were analyzed on 1% agarose gel. Lane 1: 1kb ladder, lane 2: 200ng p98 original double-stranded plasmid, Lane 3: digested 200ng p98 with EcoRI enzyme, Lane 4: digested 200ng p98 with EcoRI (control), Lane 5: digested 200ng p98 with BamHI enzyme, Lane 6: digested 200ng p98 with BamHI enzyme (control).

References

1. Gillet, L. C., Schärer, O. D., Molecular Mechanisms of Mammalian Global Genome nucleotide excision repair, *Chem. Rev.,* **2006**, *106*, 253-276.

2. Friedberg, E. C., Walker, G. C., Siede, R.D., Wood, R.A., Schultz, T. E., *DNA Repair and Mutagenesis*, 2nd edition ed., ASM Press, Washington DC, **2005.**

3. Reed, S. H., Nucleotide excision repair in chromatin: Damage removal at the drop of a HAT, *DNA Repair,* **2011**, *10*, 734-742.

4. Schärer, O. D., Chemistry and Biology of DNA repair, *Angew. Chem. Int. Ed.,* **2003**, *42*, 2946-2974.

5. Novarina, D., Amara, F., Lazzaro, F., Plevani, P., Muzi-Falconi, M., Mind the gap: Keeping UV lesions in check, *DNA Repair,* **2011**, *10*, 751-759.

6. Hanawalt, P. C., Spivak, G., Tanscription-coupled DNA repair: two decades of progress and surprises, *Nat. Rev. Mol. Cell. Biol.,* **2008**, *9*, 958-970.

7. Svejstrup, J. Q., Mechnisms of Transcription Coupled DNA repair, *Nat. Rev. Mol. Cel. Biol.,* **2002**, *3*, 21-29.

8. Lehman, A. R., DNA repair-deficient diseases, xeroderma pigmentosum, Cockayne syndrome and trichothiodystrophy. *Biochimie,* **2003**, *85*, 1101-1111.

9. Lagerweft, S., Vrouwe, M. G., Overmeer, R. M., Fousteri, M. I., Mullenders, L. H. F., DNA damage response and transcription, *DNA repair,* **2011**, *10*, 743-750.

10. Volker, M., Moné, M. J., Karmakar, P., van Hoffen, A., Schul, W., Vermuelen, W., Hoejimakers, J. H., van Driel, R., van Zeeland, A. A., Mullenders, L. H., Sequential Assembly of the Nucleotide Excision Repair Factors In Vivo, *Mol. Cell*, **2001**, *8*, 213-224.

11. Sugasawa, K., Ng, J. M., Masutani, C., Iwai, S., van der Spek, P. J, Eker, A. P., Hanaoka, F., Bootsma, D., Hoeijimakers, J. H., Xeroderma pigmentosum group C protein complex is the initiator of global genome nucleotide excision repair, *Mol. Cell,* **1998**, *2*, 223-232.

12. Sugasawa, K., Okamoto, T., Shimizu, Y., Masutani, C., Iwai, S., Hanaoka, F., A multistep damage recognition mechanism for global genomic nucleotide excision repair, *Genes Dev.,* **2001**, *15*, 507-521.

13. Sugasawa, K., Okuda, Y., Saijo, M., Nishi, R., Masuda, N., Chu, G., Mori, T., Iwai, S., Tanaka, K., Tanaka, K., Hanaoka, F., UV-induced ubiquitylation of XPC protein mediated by UV-DDB-ubiquitin ligase complex, *Cell,* **2005**, *121*, 387-400.

14. Min, J. H. and Pavletich, N. P., Recognition of DNA damage by the Rad4 nucleotide excision repair protein, *Nature,* **2007**, *449*, 570- 575.

15. Evans, E., Moggs, J. G., Hwang, J. R., Egly, J. M., Wood, R. D., Mechanism of open complex and dual incision formation by human nucleotide excision repair factors, *Embo J.,* **1997**, *16*, 6559-6573.

16. Naegeli, H., Sugasawa, K., The xeroderma pigmentosum pathway: Decision tree analysis of DNA quality, *DNA Repair*, **2011**, *10*, 673-683.

17. Wakasugi, M., Sancar, A., Assembly subunit composition, and footprint of human DNA repair excision nuclease, *Proc. NatI. Acad. Sci. USA,* **1998**, *95*, 6669-6694.

18. de Laat, W. L., Appledoorn, E., Sugasawa, K., Weterings, E., Jaspers, N.G., Hoeijmakers, J. H., DNA-binding polarity of human replication protein A positions nucleases in nucleotide excision repair, *Gene Dev.,* **1998**, *12*, 2598-2609.

19. Orelli, B., McClendon, B. T., Tsodikov, O. V., Ellenberger, T., Niedernhofer, L. J., Schärer, O. D., The interaction between ERCC1 and XPA is required for nucleotide excision repair, but not other DNA repair pathways, *J. Biol. Chem.,* **2010**, *285*, 3705-2712.

20. Dunand-Sauthier, I., Hohl, M., Thorel, F., Jaquier-Gubler, P., Clarkson, S. G., Schärer, O. D., The spacer region of XPG mediates recruitment to nucleotide excision repair complexes and determines substrate specificity, *J. Biol. Chem.,* 2005, *280*, 7030-7037.

21. Hohl, M., Thorel, F., Clarkson, S. G., Schärer, O. D., Structural Determinants for Substrate Binding and Catalysis by the Structure-specific Endonucleases XPG, *J. Biol. Chem.,* **2003**, *21*, 19500-19508.

22. Enzlin, J. H., Schärer, O. D., The active site of XPF-ERCC1 forms a highly conserved nuclease motif, *Embo J.,* **2002**, *21*, 2045-2053.

23. Staresincic, L., Fagbemi, A. F., Enzlin, J. H., Gourdin, A. M., Wijgers, N., Dunand-Sauthier, I., Giglia-Mari, G., Clarkson, S. G., Vermeulen, W., Schärer, O. D., Coordination of dual incision and repair synthesis in human nucleotide excision repair, *Embo J.,* **2009**, *28*, 1111-1120.

24. Lehmann, A. R., DNA polymerases and repair synthesis in NER in human cells, *DNA Repair*, **2011**, *10*, 730-733.

25. Gunz, D., Hess, M.T., Naegeli, H., Recognition of DNA adducts by human nucleotide excision repair, evidence for a thermodynamic probing mechanism, *J. Mol. Biol*., **1996**, *271*, 25089-25098.

26. Hess M. T., Schwitter, U., Petretta, M., Giese, B., and Naegeli H., Bipartite substrate discrimination by human nucleotide excision repair, *Proc. Natl. Acad. Sci. USA,* **1997**, *94*, 6664-6669.

27. Reardon, J. T., Sancar, A., Purification and characterization of Escherichia coli and human nucleotide excision repair enzyme systems, *Methods Enzymol.,* 2006, *408*, 189-213.

28. Shivji, M. K., Moggs, J. G., Kuraoka, I., Wood, R. D., Dual-incision assays for nucleotide excision repair using DNA with a lesion at a specific site, *Methods Mol. Biol.,* **1999**, *113*, 373-392.

29. Gillet, L.C., New photoreactive DNA substrates to study damage recognition in Nucelotide Excision Repair, Ph.D. dissertation, **2005**.

30. Sijbers, A. M., de Laat, W. L., Ariza, R. R., Biggerstaff, M., Wei, Y. F., Moggs,J. G., Carter, K. C., Shell, B. K., Evans, E., de Jong, M. C., Rademakers, S., de Rooij, J., Jaspers, N. G., Hoeijmakers, J. H., Wood, R. D., Xeroderma pigmentosum group F caused by a defect in a structure-specific DNA repair endonuclease, *Cell*, **1996,** *86*, 811-822.

31. Agard, N. J., Baskin, J. M., Prescher, J. A., Lo, A. and Bertozzi, C. R., A Comparative Study of Bioorthogonal Reactions with Azides, *ACS Chemical Biology*, **2006**, *10*, 644-648.

32. Rostovtsrv, V. V., Green, L. G., Fokin, V. V., Sharpless, K. B., A Stepwise Huisgen Cycloaddition Process: Copper (I)-Catalyzed Regioselective Ligation of Azides and Terminal Alkynes, *Angew. Chem. Int. Ed.*, **2002**, *41*, 2596-2599.

33. Prescher, J. A., Bertozzi, C. R., Chemistry in living systems, *Nat. Chem. Biol.,* **2005**, *1*, 13-21

34. Best, M. D., Click Chemistry and Bioorthogonal Reactions: Unprecedented Selectivity in the Labeling of Biological Molecules, *Biochemistry*, **2009**, *48*, 6571-6584.

35. Seela, F., Sirivolu, V.R., Chittepu, P., Modification of DNA with octadiynyl side chains: synthesis, base pairing, and formation of fluorescent coumarin dye conjugates of four nucleobases by the alkyne-azide "click" reaction, *Bioconjug. Chem.*,**2008**, *19*, 211-224.

36. Yeo, J. E., Study of Recognition Step and Repair Efficiency in Human Nucleotide Excision Repair, Ph.D. dissertation, **2011**.

37. Dey, S., Sheppard, T. L., Ketone-DNA: A versatile Postsynthetic DNA Decoration Platform, *Org. Lett.,* **2001**, *3*, 3983-3986.

38. Singh, Y., Edupuganti, O. P., Villien, M., Defrancq, É., Dumy, P., The oxime bond formation as a useful tool for the preparation of oligonucleotide conjugates, *C. R. Chimie,* **2005**, *8*, 789-796.

39. Proudnikov, D., Mirzabekov, A., Chemical methods of DNA and RNA fluorescent labeling, *Nucleic Acids Res.,* **1996**, *24*, 4532-4535.

40. Zatsepin, T. S., Stetsenko, D. A., Gait, M. J., Oretskaya, T. S., Synthesis of DNA conjugates by solid-phase fragment condensation via aldehyde-nucleophile coupling, *Tetrahedron Lett.*, **2005**, *46*, 3191-3195.

41. Angelov, T., Guainazzi, A., Schärer, O. D., Generation of DNA Interstrand Cross-Links by Post-Synthetic Reductive Amination, *Org. Lett*., **2009**, *11*, 661-664.

42. Guainazzi, A., Campbell A. J., Angelov, T., Simmerling, C., Schärer, O. D., Synthesis and molecular modeling of a nitrogen mustard DNA interstrand crosslink, *Chem.–Eur. J.,* **2010**, *40*, 12100-12103.

43. Gierlich, J., Burley, G. A., Gramlich, P. M. E., Hammond, D. M., and Carell, T., Click chemistry as a reliable method for the high-density postsynthetic functionalization of alkyne-modified DNA, *Org. Lett*., **2006**, *8*, 3639-3642.

44. Gillet, L.C., Alzeer, J., Schärer, O.D., Site-specific incorporation of N-(deoxyguanosin-8-yl)-2-acetylaminofluorene (dG-AAF) into oligonucleotides using modified 'ultra-mild' DNA synthesis, *Nucleic Acids Res.,* **2005**, *33*, 1961-1969

45. Chan, T. R., Hilgraf, R., Sharpless, K. B., and Fokin, V. V., Polytriazoles as Copper (I)-Stabilizing Ligands in Catalysis, *Org. Lett*., **2004**, *6*, 2853-2855.

46. Hong, V., Presolski, S. I., Ma, C., and Finn, M. G., Analysis and Optimization of Copper-Catalyzed Azide-Alkyne Cycloaddition for Bioconjugation, *Angew. Chem. Int. Ed*., **2009**, *48*, 9879-9883.